THERMOMECHANICAL MODELING OF A SHAPE MEMORY POLYMER

A Thesis

by

PRITHA GHOSH

Submitted to the Office of Graduate Studies of
Texas A&M University
in partial fulfillment of the requirements for the degree of

MASTER OF SCIENCE

December 2008

Major Subject: Mechanical Engineering

THERMOMECHANICAL MODELING OF A SHAPE MEMORY POLYMER

A Thesis

by

PRITHA GHOSH

Submitted to the Office of Graduate Studies of
Texas A&M University
in partial fulfillment of the requirements for the degree of

MASTER OF SCIENCE

Approved by:

Chair of Committee,	Arun Srinivasa
Committee Members,	William Schneider
	Jay Walton
Head of Department,	Dennis O'Neal

December 2008

Major Subject: Mechanical Engineering

ABSTRACT

Thermomechanical Modeling of a Shape Memory Polymer. (December 2008)

Pritha Ghosh, B.E., Govt. College of Engineering Pune, India

Chair of Advisory Committee: Dr. Arun Srinivasa

The aim of this work is to demonstrate a Helmholtz potential based approach for the development of the constitutive equations for a shape memory polymer undergoing a thermomechanical cycle. The approach is motivated by the use of a simple spring-dashpot type analogy and the resulting equations are classified as state-equations and suitable kinetic equations for the recoverable-energy elements and the dissipative elements in the model respectively. These elements have mechanical properties which vary with temperature. The governing equations of the model are developed starting from the basic conservation laws together with the laws of thermodynamics. The entire set of equations are written in a state-evolution form as a set of ordinary differential equations to be solved using Matlab. It is shown that the results of the simulation in Matlab are in qualitative and quantitative agreement with experiments performed on polyurethane. Subsequently, we study the dependence of the yield-stress on temperature to be similar and different functions of heating or cooling processes.

ACKNOWLEDGMENTS

Dr. Arun Srinivasa has been the motivation for this work. His teaching style has been an eye-opener for me at various levels: rigor in mathematics, logic in thinking and lucidity in expression. One of our discussions when we first started work on this project digressed to *having biases in science*, leading to having goal-oriented approaches rather than learning for pleasure. I still remember him laughing at my dilemmas and saying "learning science is like taking a walk through a garden. Explore and enjoy. Don't take things too seriously because in the end you're going to die!" I hope I shall be able attain this fine balance of attachment and detachment with my work. I have enjoyed working with him and am glad that I shall continue to do so.

I extend sincere thanks to my committee members: Dr. Walton's austere method of teaching Tensor Analysis helped me overcome certain obstacles I faced ever since I was first introduced to tensors in 2006. I thoroughly enjoyed Dr. Schneider's course on Advanced Strength of Materials, his exams being some of the toughest and most satisfying that I have encountered.

Thanks are also due to few of my friends at Texas A&M who have been generous with their time. Discussions with Saradhi Koneru, Shriram Srinivasan and Satish Karra have helped at various levels in this work ranging from Mechanics and Thermodynamics to Matlab and Latex as well! Thank you Anand Govindasamy and Abhilasha Katariya for your "timely" pearls of wisdom! A special thank you to Anjana Talapatra for seeing me through extremes of moods in the last few months of this work, and having an extra-ordinary capacity to make things look "just fine"!

Finally, I owe a special mention of my family who persuaded me to go ahead and begin work for a Master's degree. I thank Pa-Da-Ma for their efforts and patience!

TABLE OF CONTENTS

CHAPTER Page

LIST OF TABLES

LIST OF FIGURES

FIGURE Page

FIGURE Page

CHAPTER I

INTRODUCTION

A. Introduction

Shape memory polymers belong to a class of smart materials, that have the ability to "remember" their original shape. A shape memory polymer deforms into a temporary shape and returns to its original shape by external environmental stimuli such as chemicals, temperature or pH. Temperature-responsive shape memory polymers are those that undergo a structural changes at a certain temperature called the transition temperature. This transition temperature could correspond to glass-transition or the melting temperature, which gives rise to different kinds of shape-memory polymers[1]. They can be easily deformed to give a temporary shape at low-working temperatures and upon heating return to their original structure. Examples of shape memory polymers are polyurethanes, polyurethanes with ionic or mesogenic components, block copolymers consisting of polyethyleneterephthalate and polyethyleneoxide, block copolymers containing polystyrene and polybutadiene, polyesterurethanes with methylenebis and butanediol [1]. These polymers are currently being investigated for a wide range of applications where their shape fixity and shape recovery behavior are useful. Theories of such shape fixity behavior have been developed by Tobushi et.al. [2] [3] [4] [5], Abrahamson et.al.[6], Takahashi et. al.[7], Lee, Kim et. al. [8], Lin and Chen [9], Bhattacharyya and Tobushi [10], Hong et. al. [11], Liu et. al. [12] [13].

The chief objective of this work is to simulate the behavior of a shape memory polymer using a a thermodynamically consistent model that will capture the response

---

The journal model is *IEEE Transactions on Automatic Control.*

of these polymers. The equations of the model are given in state-space form rather than as integral equations, which are more common in non-linear viscoelasticity literature. This form allows the model to be conveniently incorporated into control strategies.

We demonstrate that a systematic application of fundamental thermodynamic principles coupled with a suitable choice for the Helmholtz potential and suitable kinetic equations for the inelastic variables will allow the development of a complete simulation of the behavior of shape memory polymeric materials. The second objective is to compare the obtained results with the experimental data, from the work of Tobushi et. al. [3] for a polyurethane-polypol sample. The development of the model is done such that it allows the constitutive behavior to be incorporated into a toolbox like MATLAB.

B. Applications of Shape Memory Polymers

Shape memory polymers (SMPs) have been available since the 1980s because of their central feature of being able to change their shape to a useful predefined one, in response to stimuli. This feature can be exploited to design components that are used to enhance product performance and quality under changeable environments. Due to some of the unique thermomechanical properties, as discussed in section 3, shape memory polymers have found numerous applications (see Figure (1)). Before we discuss specific examples, we would like to emphasize that the key aspect to the use of shape memory polymers is the large recoverable change in properties across a narrow temperature range. This can be used to monitor and actuate various mechanisms.

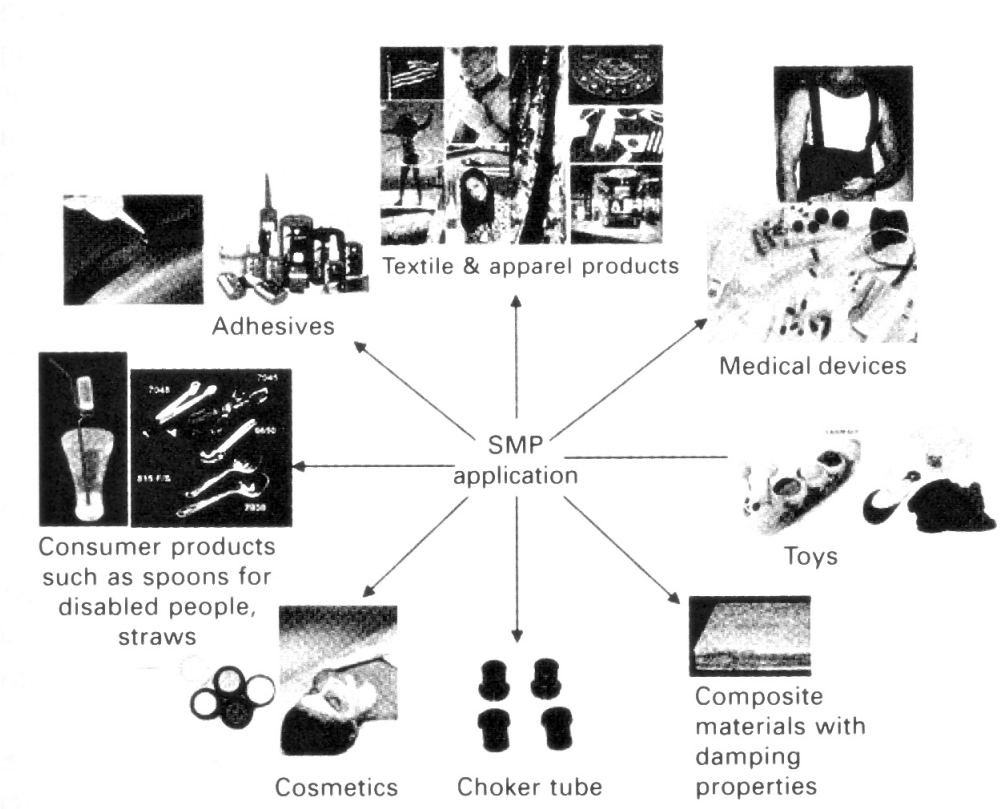

Fig. 1. Applications of the SMP[18].

For example:

1. **Change in Shape**

   The thermal transition of many SMPs occurs in the temperature range from room temperature to body temperature. This can be exploited in biomedical applications. SMPs can be made both compatible with the body and biodegradable upon interaction with physiological environment as studied by Lendlien and Langer [14] and their team to produce scaffolds for engineering new organs and coronary stents. Many SMPs, when deformed at low temperature,tend to retain their deformed shape and recover upon heating above the glass transition.

Such stents could be compressed and fed through a tiny hole in the body into the blocked artery. Then, the warmth of the body would trigger the polymer's expansion into original shape. Instead of requiring a second surgery to remove the SMPs, the polymer would gradually dissolve in the body.

Fig. (2) shows (a) A smart surgical suture self-tightening at elevated temper-

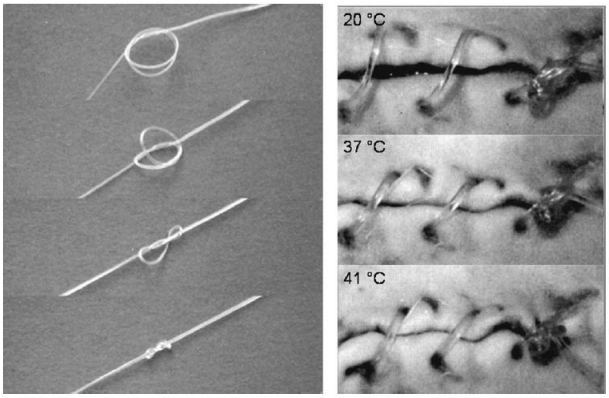

Fig. 2. Example of an application of SMP - Surgical Sutures [17].

atures (left). A thermoplastic shape-memory polymer fiber was programmed by stretching to about 200% at a high temperature and fixing the temporary shape by cooling. After forming a loose knot, both ends of the suture were fixed. The photo series shows, from top to bottom, how the knot tightened in 20 s when heated to 40 °C. (b) Degradable shape-memory suture for wound closure (right). The photo series from the animal experiment shows (top to bottom) the shrinkage of the fiber while the temperature increases from 20 to 41 °C.

2. **Changes in Elastic Modulus**

The large temperature dependence of the elastic modulus can be utilized to make temperature sensors, as investigated by Ni, Zhang et. al for SMP nanocom-

posites [15].

3. **Change in Moisture Permeability**

   The temperature dependent moisture permeability of a thin film can be used on fabrication of sport clothing. Moisture permeability for such thin films is high above glass transition and low below it. Shape memory fabrics have recovered their original flat appearance, and retained the original creases designed into them, after the fabrics have been immersed in water[16].

Apart from these examples, research has been carried out on the innovative applications of shape memory polymers in other areas including biomedical devices, spatial deployment structures and engineering buckling control systems. Despite the early discovery of SMPs in the early 40s, recognition of the importance of shape-memory polymers did not occur until the 1960s in the form of heat shrinkable tubes using covalently cross-linked polyethylene. Significant industrial end-application oriented efforts began in the late 80s and this trend continues to grow as shown by the number of publications appearing yearly, which is summarized in Figure (3). Approximately 40% of these have been published by Japanese researchers. Research in this area accelerated in the 1990s, and the mechanics of why the material behaves this way found interest in academia. The trend has kept growing since then, especially the total publication numbers, as reported in a recent review article by Liu and Qin [17] in 2007. Lendlien and Kelch[1] comment that despite the development of SMPs, few applications have been implemented since only a few shape-memory polymers have so far been investigated and even less are available on the market. Extensive innovations have to be anticipated because of the interesting economical prospects that have already been realized for the shape-memory technology within a short time period.

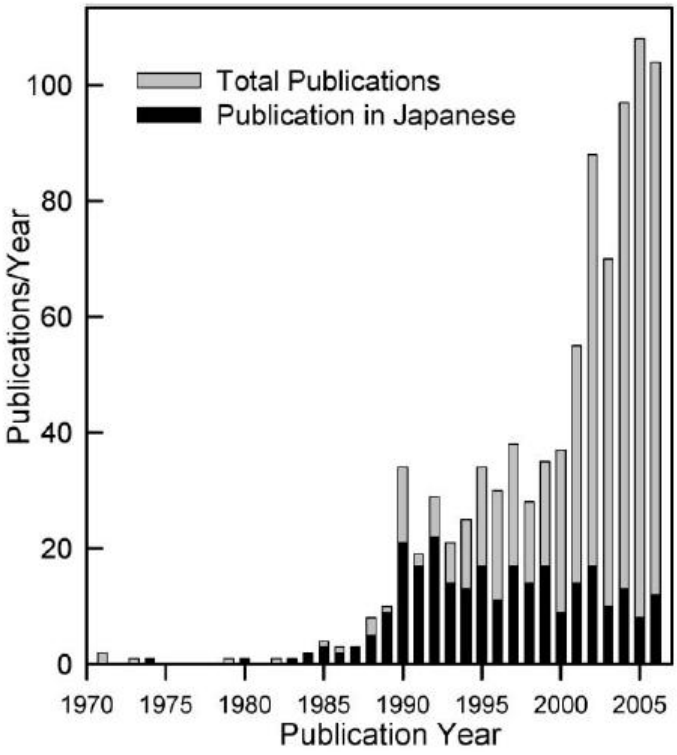

Fig. 3. Publication history of SMPs from 1970 to 2006 [17].

Hu[18] predicts that SMP features could be engineered into most polymers by late 2020s. For example automobile fenders could be bent back into their original shape by the right amount of heat; multi-form solid furniture could be transformed into shape-accommodating ones for different users by simply pressing a button!

C. Physics of the Shape Memory Polymer

1. Shape Memory Deformation Process

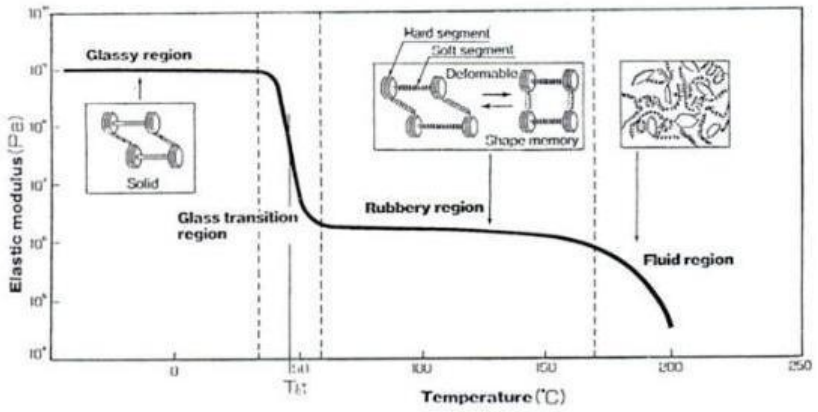

Fig. 4. Variation of elastic modulus of the SMP across glass transition temperature.

Shape memory polymers allow large reversible change in properties across the glass transition temperature (θ_g). The glass transition temperature, θ_g, is the temperature at which a polymer, becomes brittle on cooling, or soft on heating. For example, the material can change from a glassy state to a rubbery state across the θ_g, because of a change in its modulus, as show in Fig. (4). Allowing a large change in elastic modulus around the θ_g temperature, significant deformation occurs in response to temperature changes. An increase in temperature allows the material to become more flexible, therefore easily deformed, and a decrease in temperature hardens the plastic sustaining the new shape, as studied by Rogers, 1990 [19]. It is important to note that the glass transition temperature is a kinetic parameter, and thus depends on the melt cooling rate. Thus the slower the melt cooling rate, the lower θ_g.

Lendlien and Kelch, 2002 [1] assert that "the shape memory effect in polymers

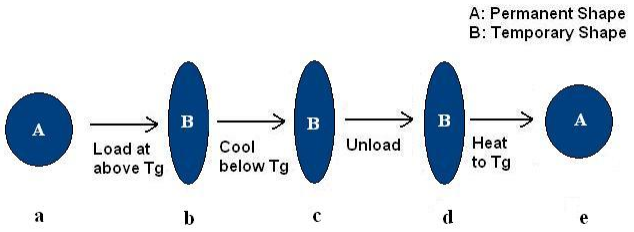

Fig. 5. Schematic diagram of the deformation process in a shape memory material.

results from a combination of the polymer structure and the polymer morphology together with the applied processing and programming technology."

The process of programming and recovery of a shape is shown schematically in Figure (5). First, the polymer is processed to receive its permanent shape "A" as shown in Fig. (5.a) at a temperature above its glass transition. Then, the polymer is deformed and the intended temporary shape "B" is fixed as in (5.b). The polymer is then cooled to below its glass transition temperature (5.c), and unloaded (5.d). It is seen that the material retains to the new shape "B" imparted to it, as long as this low temperature is held. On heating the polymer above a transition temperature, the permanent shape "A" is regained once again as shown in (5.e). This is the general outline of the deformation mechanism observed in most shape memory polymers.

2. Structure of Shape Memory Polymers

Most of the shape memory effects are based on the existence of separated phases related to the coiled polymer structure, cross-links, hydrogen bonding, etc. In terms of

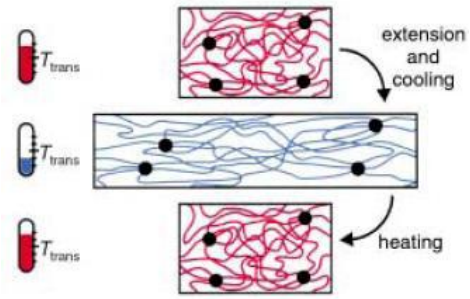

Fig. 6. Morphology change in an SMP at different temperatures.

chemical structure, SMPs can be considered as phase-segregated linear block copolymers having a hard segment and a soft segment. The hard segment acts as the frozen phase and the soft segment acts as the reversible phase. The reversible phase transformation of the soft segment is responsible for the shape memory effect. Shape memory polymers are processed to have a permanent 'parent' shape by molding. The polymer assumes different temporary shapes, and by heating the polymer higher than the transition temperature, the permanent shape can be restored.

The phase corresponding to the higher transition polymer component acts as the cross-links responsible for the permanent shape, as shown by the black dots in Fig. (6). The second component shown by the red lines in the figure, acts the 'molecular switch' and helps to "freeze" temporary shapes below the transition temperature, with either glass transition temperature or the melting temperature serving as the transition/switching temperature. The temporary configuration attained by the second component is shown in blue lines. Temporary shapes can thus be formed above the switching temperature and can be frozen by keeping the material below the switching temperature, while the permanent shape can be obtained again by heating above the switching temperature. This is the reason why most of the thermally induced SMPs have a "one-way" shape memory effect: they remember one permanent shape formed at the higher temperature, while many temporary shapes are possible at lower temperatures for which the systems do not have any memory. Lendlein and Kelch [1] observed that the shape memory effect could be controlled by a thermomechanical cycle. In the following section, we shall discuss how this controls the strain recovery of the SMP.

3. Experimental Procedure and Related Mechanical Properties of SMPs

The experiment that we shall be considering in this work is a thermomechanical cycle on a shape memory polymer as shown in Figure (7) from the work carried out by Tobushi, Hayashi et al. [3]:

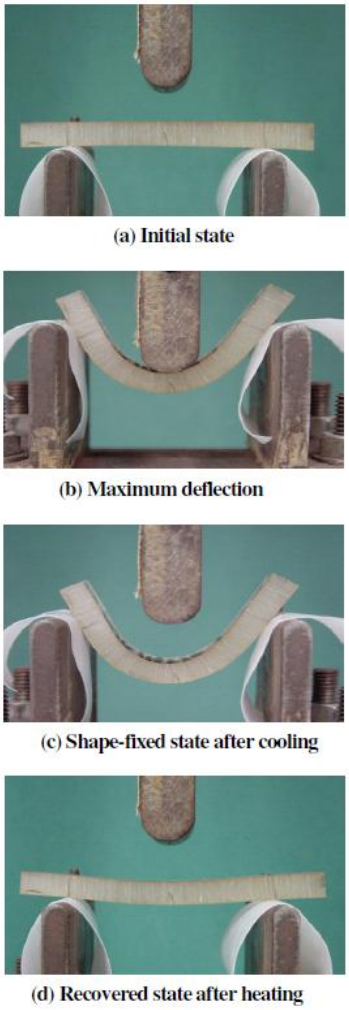

Fig. 7. Experiment under study for the SMP: The processes taking place in a thermomechanical cycle [5].

The process involved here are:

1. *Initial conditions:* The material is considered at a stress free state at a temperature above the glass transition temperature $\theta_g = \theta_g + 20$. All strains are to be measured from this state. This current shape is thus recognized as the permanent shape of the material.

2. *Process A: High temperature stretching*: The temperature is held fixed at θ_{max} and the strain is increased steadily at a constant prescribed rate g_1 to give the temporary shape to the material, and then the strain is held constant for a time $0 < t < t_1$.

3. *Process B:Cooling and Fixing the temporary shape*: The strain is fixed at g_1 and the temperature is lowered to $\theta_{min} = \theta_g - 20$ at a predetermined rate 'a'.

4. *Process C: Relaxing the stress*: Now the temperature is fixed at θ_{min} and the stress is gradually relaxed to zero at a predetermined rate $b < 0$. During this process, material is observed to still be in its new temporary shape.

5. *Process: D Recovering the original shape*: Now the body is heated at rate 'a' in a stress-free state back to the original temperature to recover the original shape. The strain slowly relaxes and the material is back to its original shape.

To characterize the shape memory properties of polymers, a set of parameters is needed which reflect the nature of the polymer response, differentiate the SME from other properties of the material, and define the shape memory process. In view of these factors, some parameters have been proposed and quantified (Hu, 2007 [18]) with respect to the experiment described above.

1. ***Shape fixity:***

   This parameter was proposed to describe the extent to a temporary shape is

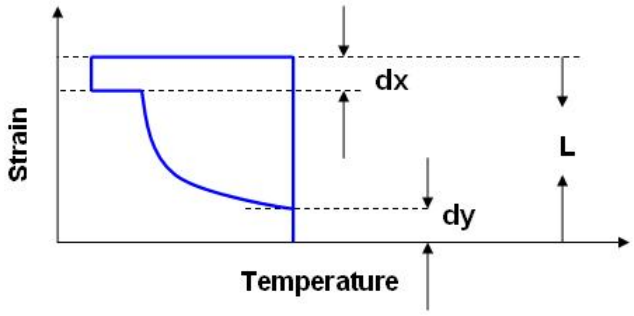

Fig. 8. Strain response in a thermomechanical cycle.

fixed in one cycle of shape memorization. Refer to Fig. (8), the extent of temporary shape being fixed is (L - dx), where dx is the amount by which the material recovers at the end of unloading, and L is the total deformation.

Shape fixity = $\frac{\text{L - dx}}{\text{L}} \times$ 100 percent

Shape fixity is related to both structures of polymers and the thermomechanical conditions of shape memorization.

2. ***Shape recovery:***

Shape recovery (R_r) is used to reflect how well the permanent shape is recovered. Refer to Fig. (8), the amount of recovery of permanent shape is ($L - dy$).

Strain recovery = $\frac{\text{L - dy}}{\text{L}} \times$ 100 percent

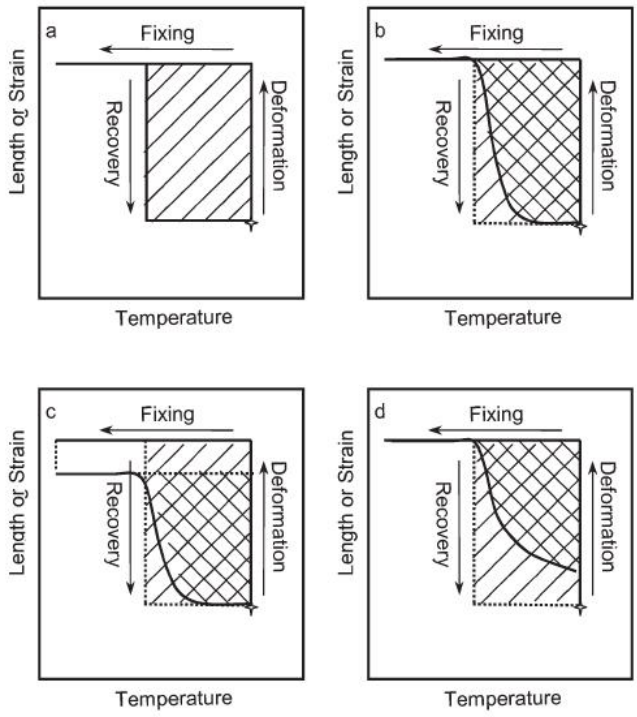

Fig. 9. Classifications of shape-memory polymers by their shape-fixing and shape-recovery abilities [17].

Using the above definitions helps classify material behavior as shown in Fig. (9). Fig. (9.a) shows an ideal shape-memory material; Fig. (9.b) shows a shape-memory material with excellent shape fixing and shape recovery; Fig. (9.c) shows a shape-memory material with excellent shape recovery but poor shape fixing; and Fig. (9.d) shows a shape-memory material with attractive shape fixing but poor shape recovery.

Table I. Classification of Previous Efforts in Modeling SMPs

<table>
<tr><th>Type/Approach</th><th>Empirical</th><th>Spring-dashpot</th><th>Thermodynamics</th></tr>
<tr><td rowspan="2">Rate Type Model</td><td rowspan="2"></td><td>Tobushi, Hashimoto [3]
Bhatacharyya [10]
Abrahamson [6]
Lin and Chen [9]
Li and Larock [20]</td><td>Liu, Gall et.al[12]
Diani et. al [13]</td></tr>
<tr><td colspan="2">Our Model</td></tr>
<tr><td>Integral Model</td><td>Hong and Yu [11]</td><td></td><td></td></tr>
</table>

D. Modeling Efforts of the SMP Response

Brief Review of the Literature on Shape Memory polymers

The literature on the shape-memory effect (SME) in polymers mostly deal with the development of theoretical concepts of the mechanisms of thermally stimulated strain recovery [5]; new approaches to the description of the deformation and relaxation behavior of polymers [7]; new information on the shape recovery features of deformed samples; and results of investigations of synthetic polymeric materials possessing unusual properties [21]. In a recent article[12] Liu and Gall state that relatively little work in the literature has addressed the *constitutive modeling* of the unique thermomechanical coupling in SMPs. They emphasize that constitutive models are critical for predicting the deformation and recovery of SMPs under a range of different constraints. Table (I) shows a classification of various kinds of models developed for SMPs based on their approach. The shape memory behavior is dependent on both the structure and the thermomechanical conditions. Establishing appropriate models

to simulate the shape memory processes and therefore to predict the shape memory properties should be helpful for the development and application of SMPs. The current models for SMPs have all been established on the basis of viscoelasticity of polymers, i.e the shape memory behaviors of the SMPs are ascribed to the changes of viscoelastic properties.

1. Model Proposed by J. R. Lin

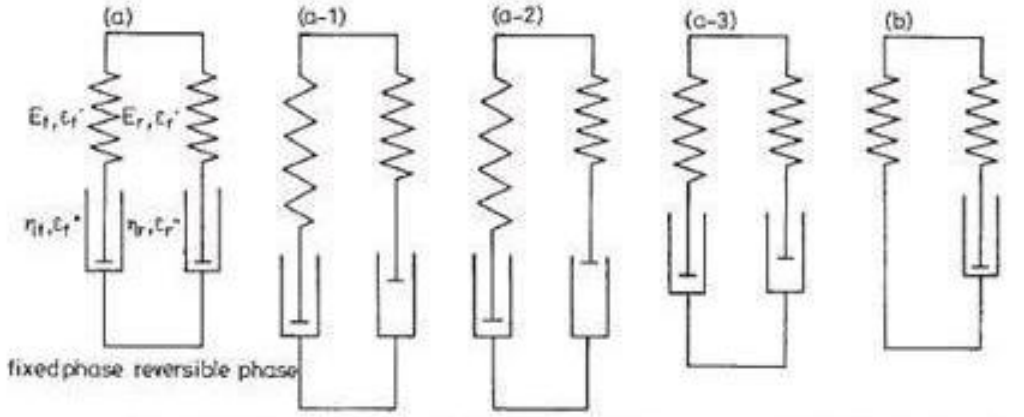

The viscoelastic model and mechanism of shape-memory polymer: (a) the general model of shape-memory polymer; (b) the simplified model of the crosslinked shape-memory polymer; (a-1) deformed to ε_0 at T_1; (a-2) kept the strain ε_0 at T_1 for a long time, then cooled to T_2, followed by a release of the external force; (a-3) heated at the rate of $T = T_2 + at$ and, after heating, the model recovers to its original state.

Fig. 10. Model proposed by Lin and Chen.

As Fig. (10) shows, the authors [9] employed two Maxwell models connected in parallel to describe the shape memory properties of some shape memory polyurethane (SMPU). The left side represents the fixed phase and the right is the reversible phase. The changes of the model in a whole cycle of shape memory processes are shown.

At a high temperature (e.g. $T_L < T_1 = 80°C < T_H$), the model was stretched

to a constant strain and maintained this constant strain as shown in Fig. (10.a-1). The mechanical parameters of the model were derived as a function of time (t) and temperature (T). The modulus E(t, T) and stress s(t, T) of the model are expressed as follows:

$E(t,T) = E_f(T)$ X $exp[-t/\tau_f(T)] + E_r(T)$ X $exp[-t/\tau_f(T)]$

$\sigma(t,T) = \epsilon_0$ X $[E_f(T)$ X $exp[-t/\tau_f(T)] + E_r(T)$ X $exp[-t/\tau_f(T)]]$

τ_f: relaxation time for fixed phase

τ_r: relaxation time for reversible phase

The model simplifies to that shown in Fig. (10.b), which is a Kelvin-Voigt model.

The modeling results and experimental data as shown in Fig. (11), show some

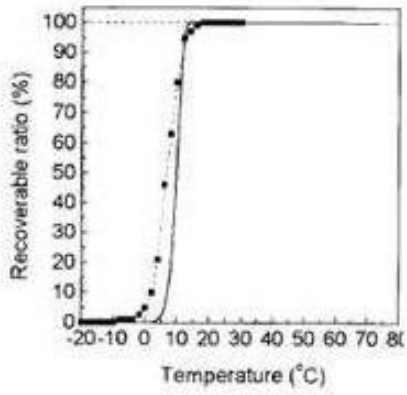

Comparison of the shape memory behavior between the model (solid line) and the experimental data (dotted line)

Fig. 11. Results of the model proposed by Lin and Chen.

deviation, which Lin and Chen ascribed to the polydispersed T_g of the studies samples. The model can qualitatively explain the occurrence of shape memory behaviors. Below the transition temperature, the molecular motion of the reversible phase is

frozen, while above it, it is activated. Thus the model is suitable for chemically cross-linked SMPUs. But whether it is suitable for physically cross-linked SMPUs is still uncertain. Since the dampers in the model are both viscous, there is no irrecoverable strain at the end of the process. Furthermore, the model was not developed using thermodynamical principles and so it is impossible to incorporate the understanding of the underlying physics of the process into the model, and thus does not provide any guidance as to how materials can be designed with properties that are useful.

2. Model Proposed by H. Tobushi

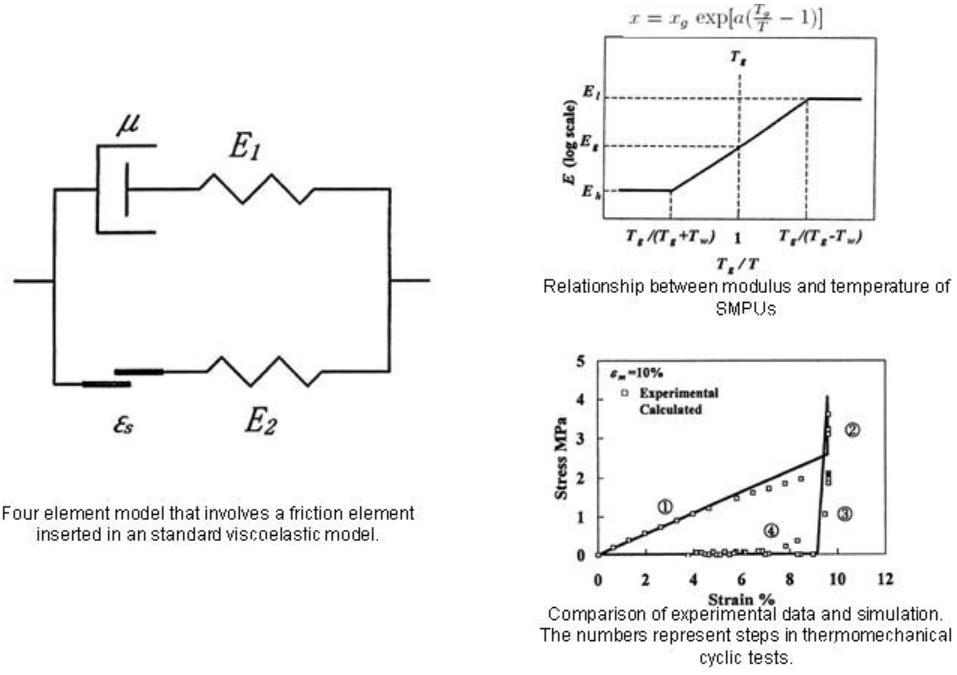

Fig. 12. Model proposed by Tobushi.

Compared with [9], the H. Tobushi Model [3] takes irreversible deformation into account. Tobushi and coworkers added a friction element into the standard linear viscoelastic (SLV) model as shown in Fig. (12.a) to simulate the behaviors of SMPUs.

They carried out a series of creep tests of SMPUs at different temperatures. It was found that every temperature corresponded to a particular threshold strain $\epsilon_L(T)$. When the strain is below $\epsilon_L(T)$, there is no irreversible deformation. But if the strain exceeds $\epsilon_L(T)$, the irreversible deformation occurs. Tobushi et. al. accounted for it by introducing dry friction into the model. Also, the temperature change that would cause thermal expansion was accounted for in an ad hoc manner by simply adding a coefficient of thermal expansion to terms invloving the rate of strain. Finally, recognizing the fact that the SLV model is unsuitable for large deformations, the authors revised the above linear model into a non-linear one by introducing power terms in it as below:

Linear: $\dot{\epsilon} = \frac{\dot{\sigma}}{E} + \frac{\sigma}{\mu} - \frac{\epsilon - \epsilon_s}{\lambda} + \alpha\dot{T}$

Non-Linear: $\dot{\epsilon} = \frac{\dot{\sigma}}{E} + m(\frac{\sigma - \sigma_y}{k})^{m-1} + \frac{\sigma}{\mu} + \frac{1}{b}(\frac{\sigma}{\sigma_c} - 1)^n - \frac{\epsilon - \epsilon_s}{\lambda} + \alpha\dot{T}$

Tobushi also investigated the relationship of the modulus with temperature as shown in Fig. (12.b) and expressed all parameters including $\mu, \lambda, k, \sigma_y, \sigma_c,$ C andϵ_L as:

$x = x_g \exp[a(\frac{T_g}{T} - 1)]$.

Fig. (12.c) shows that the theoretical simulation agreed well with the experimental results. Tobushi's work was one of the first to attempt to match the whole thermomechanical cycle. Second, it takes into account the irreversible deformation at the end of the cycle. However this model is not related to the structure of SMPs, and it involves several parameter measurements. The validity of this model needs to be checked for large deformation amplitude. Also the model has certain thermodynamical inconsistencies which will be discussed in greater detail in Chapter III.

3. Model Proposed by E. R. Abrahamson

Abrahamson et al. [6] utilized the model shown in Fig. (13.a) to investigate the shape memory behaviors of thermosetting SMPs. A key feature is that the friction element

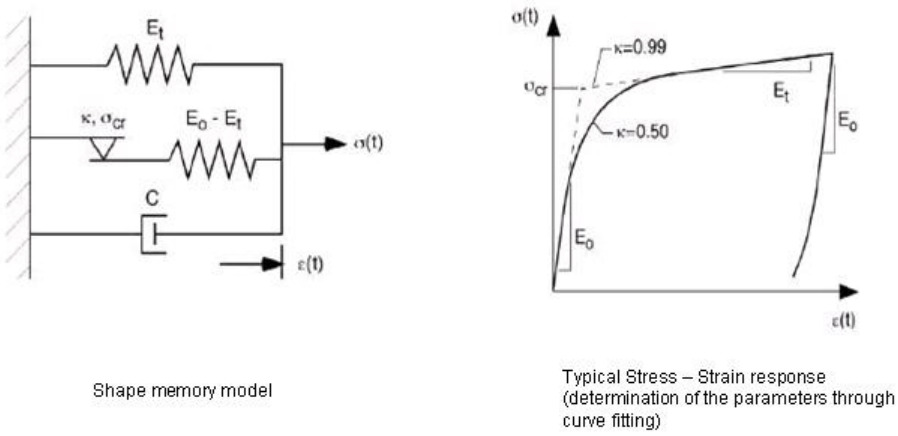

Fig. 13. Model proposed by Abrahamson.

progresses from fully stuck to fully free over a finite range of strain. The major difference between this model and its traditional application in plasticity theory is that the values for the four empirical parameters vary with temperature. The non-linear constitutive equation of the model is as below:

$$\dot{\sigma}(t) = E_0\dot{\epsilon}(t)[\frac{1+(sgn[\dot{\epsilon}(t)]/\sigma_{cr})[E_t\epsilon(t)-\sigma(t)]}{1+\kappa(sgn[\dot{\epsilon}(t)]/\sigma_{cr})[E_t\epsilon(t)-\sigma(t)]}] - C\ddot{\epsilon}(t)$$

The parameter κ controls the rate at which friction slider progresses from fully stuck to fully slipping. The parameters were determined experimentally for solving the differential equation. As shown in Fig. (13.b), the parameters were obtained through curve fitting the stress-strain curve. It was found that the stress-strain curve predicted by the model and that obtained by experiment agreed well. However, the model does not take the thermal expansion of the material into consideration during the change of temperature, and it does not consider the structural influence of SMPs.

E. Conclusion and Scope

From the foregoing discussion, the models for SMPs are all based on the polymer viscoelastic theory. The shape memory behaviors of SMPs can be qualitatively explained by the models. However, most of the models are not ideal for predicting the shape memory parameters, though Tobushi et. al. and Abrahamson et. al. have simulated the stress-strain relationship. In particular, the models only simulated the shape memory behavior in case of low deformation strain and the validity of the models for high deformation strain remains to be testified. One of the major difficulties for the modeling of SMPs is the fact that the characteristic structure of SMPs has not yet been completely revealed, i.e the relationship between the shape memory properties and structures is not fully understood. In addition, as more and more SMPs with different structures are developed, it seems impossible to simulate all the SMPs with only one model. The models studied above start with a purely mechanical analogy and convert the temperature dependent parameters in the mechanical model as a function of temperature in an ad hoc manner. Moreover, these parameters have to be specified as complex functions of temperatures, and thus it becomes exceeding difficult to evaluate these models from a design point of view.

The current work deals with the development of a thermodynamically consistent model in a state-space form and shows that most of the gross features of a SMP depend on the yield-stress of the material. The yield-stress function of the material may differ during heating and cooling depending on the glass-transition of the material during these two processes. The modulus of the material also depends on heating and cooling processes which affects the number of temporary entanglements formed, and will thus help in defining the response during heating and cooling more precisely. This however, is outside the scope of this work. Explicit history depen-

dence of the material response, and moisture absorbtion capabilities of the material will not accounted for. Although the thermal expansion of the material will be taken into consideration, SMPs being poor conductors of heat, the temperature of polymer is kept same as ambient temperature. Thus, we shall not be dealing with heat equation in this work, rather we shall take temperature changes to the material as a defined input. The effect of yield-stress being similar during heating and cooling, and being different functions of heating or cooling processes shall be shown. The yield-stress mostly affects the rate of temporary entanglements broken and reformed in the cross-linked polymer matrix, during heating and cooling. The solution of the system equations for a simple thermomechanical cycle shall be simulated in MATLAB and its results shall be shown to be in qualitative and quantitative agreement with experiments performed on polyurethane.

CHAPTER II

MECHANICAL MODEL FOR THE SMP BEHAVIOR

The only laws of matter are those that our minds must fabricate and the only laws of mind are fabricated for it by matter -James Clerk Maxwell

A. Introduction

When an external force is applied to a piece of material, the material develops the ability to produce an internal force by distortion of its underlying physical structure. Materials are classified based on their response to the external force, depending on how they change their physical structure to build the internal force. The viscoelastic behavior of a material involves qualities of both elastic solid and viscous fluid-like response as discussed by Wineman and Rajagopal [22]. This is due to the material microstructure, and is related to the movement of flexible macromolecules. Following Bland's [23] hypothesis, the microscopic structure of a linear viscoelastic material is mechanically equivalent to a network of viscous and elastic elements, without any restriction on the number of these elements or on their arrangement.

The viscoelastic mechanical response as discussed here is simulated by a spring-viscous damper combination along with a friction-element. As pointed out by Ferry [24], different viscoelastic models can be made equivalent by suitable values of the model parameters. Hence it should be remembered, that the model here is intended to be used to simulate only macroscopic behavior. It does not necessarily provide insight into the detailed molecular basis of viscoelastic response; its elements should not be thought of as corresponding directly to any molecular processes in detail, although we shall explain a few suitable analogous conclusions from the behavior observed in

the model and the experimental responses.

B. Proposed Mechanical Model

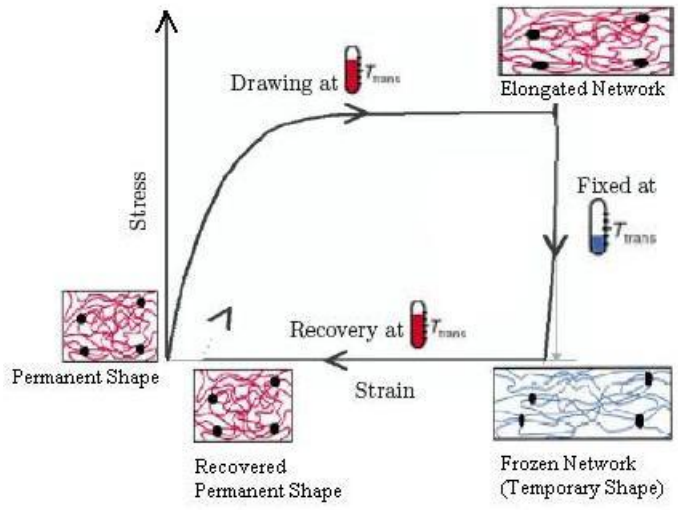

Fig. 14. The thermomechanical cycle.

In order to provide a "physically intuitive" model of SMP behavior, we now proceed to develop a simplistic "cartoon-like" model of the behavior of a shape memory polymer. The thermomechanical cycle, as described in previous chapter, Section (3), includes the following processes as shown in Fig. (14).

From (a) to (b): The polymer is stretched above θ_g.

From (b) to (c): The polymer is cooled below θ_g by applying forces to keep the shape fixed.

From (c) to (d): The forces are removed at constant low temperature and the temporary shape is retained.

From (d) to (a): The polymer is heated to above θ_g and the material rebounds back to its original shape.

Let us assume that at high enough temperatures, the response of the SMP is akin to that of an amorphous cross-linked polymer as shown in Fig. (15).

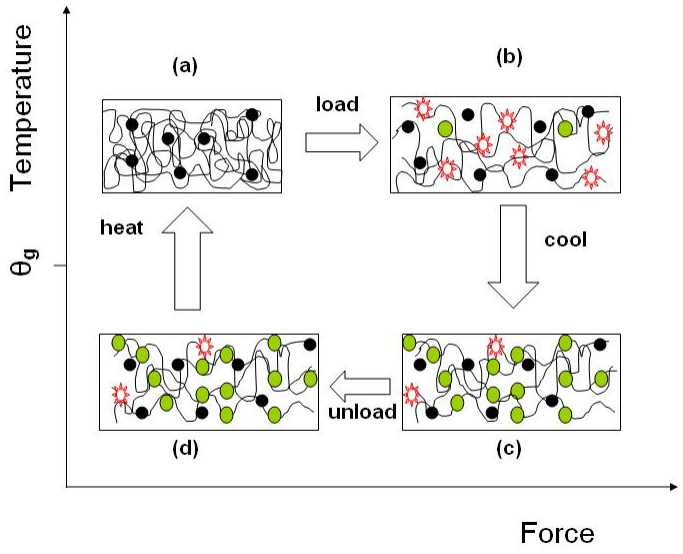

Fig. 15. A schematic representation of the shape fixing effect of a rubbery polymer around the glass transition.

To model this, we borrow ideas from multi-network theory dating back to Tobolsky and Andrews [25], and use a two-network theory; one of which is a *permanent-network* responsible for permanent shape retention and recovery while the other network is a *temporary-network* which can be made to persist over long periods of time by suitably lowering the temperature. This latter network is responsible for the shape fixing properties of the polymer at low temperatures. Furthermore the interactions

between the two networks are related to the shape fixity and shape recovery parameters which of interest.

Change in morphology from state (a) to (b): As the polymer is stretched, the permanent network deforms due to the partial uncoiling of the polymeric chains between the cross-links. These network cross-links/junctions form the permanent backbone or skeleton of the polymer and are ultimately responsible for its shape recovery at high temperature(shown as black dots in Figure (15a). There is also a sufficient amount of electrostatic attraction between the individual chains, and when two chains come close enough they stick together momentarily before breaking off. This sticking-together gives rise to what we term as 'temporary nodes', which break (shown in red circles in Figure (15b)) and reform (shown in green circles in Figure (15b)) continuously at high temperature. The connections between these temporary nodes form the temporary network.

Change in morphology from state (b) to (c): As the material is cooled, the mobility of the chains decreases and the temporary nodes that are formed are sufficient to hold parts of the chains immobile for much longer periods of time, i.e. the chains exhibit "stickiness", so much so that below a certain temperature the chains lose their rubbery character and are "frozen" [26]. The material becomes a glassy polymer. The network formed by these temporary junctions forms a second temporary network (shown in abundant green circles in Figure (15c)) that interpenetrates the first, permanent network. It is the temporary junctions that are responsible for the polymer to retain a temporary "frozen" shape upon cooling. In other words, the new junctions that are formed in the deformed state, cause the deformed state to be "locked in". The exact state of deformation that is "locked in" depends upon the relative effects of the permanent junctions (black circles) which will try to return the polymer to the original state and the temporary junctions (green circles) that try to

keep it in the deformed state. Of course, in reality, due to thermal fluctuations, the temporary junctions will occasionally break and reform, giving rise to "creep" of the polymer with time.

Change in morphology from state (c) to (d): On unloading of the material, not much changes take place in the morphology, except for slight recovery of the permanent chains. Because the external load is removed, the permanent network will have a tendency to coil back to its initial configuration. However, the temporary nodes "lock-in" the deformed state of the permanent network here as the nodes are extant at low temperatures.

Change in morphology from state (d) to (a): Subsequent heating increases the mobility of the chains, and the rate of breaking and reforming of temporary nodes starts rising once again. This"unlocks" the permanent network which now take over and recoil the polymer back to its original state.

This simple view of the material response is adequate to create a reasonable

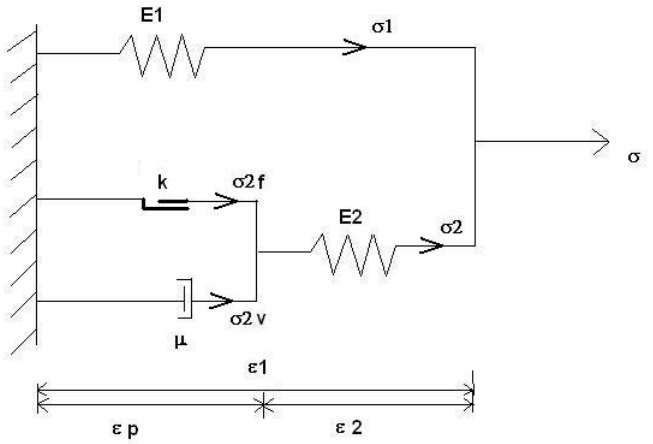

Fig. 16. The proposed mechanical model for the SMP.

macroscopic model which captures many of the features of the response of SMPs to

various thermomechanical loads. In view of this microscopic cartoon, is clear that any model that we develop should have:

(a) Two elastic modular: one which is apparent at low temperatures and another at high temperatures,

(b) "Yield" behavior which is temperature sensitive so that it allows strains to be "locked in" at low temperatures,

(c) Viscous behavior that will accommodate the sticky slippage of the temporary network chains.

The model shown in Fig. (16) represents a possible model that has many of the features mentioned in the above discussion. The model includes:

(a) Two springs : a rubbery spring and a glassy spring.

(b) A frictional element that represents the "yield" behavior. At high temperatures, the frictional element has essentially zero friction (representing the materials ability to easily break the temporary bonds, so that for all practical purposes the second spring is "slack" at high temperatures.) At low temperatures, the temporary bonds come into play and the frictional dashpot exhibits a high frictional threshold, causing the system to lock.

(c) A viscous dashpot that shall account for how long the temporary nodes sustain before breaking off. This shall also vary with temperature.

For this work, we will focus on the above model. *While it is tempting to convert this mechanical model directly into a set of response functions, it is extremely dangerous to do so, since the properties are all very sensitive to temperature in the operational range and, because of the strong thermomechanical coupling, care must be taken in maintaining thermodynamical consistency.* The approach in this work is not based on just following the mechanical analogy by making suitable changes to the temperature dependent parameters as done by other researchers in this field.

Rather, we will use the mechanical analogy as a motivation to obtain suitable forms for the Helmholtz potential and derive the response functions from thermodynamical considerations thus maintaining full thermodynamical consistency.

CHAPTER III

MODEL FORMULATION

All effects of nature are only the mathematical consequences of a small number of immutable laws -Laplace

A. Introduction

We shall be simulating the model responses as recorded by Tobushi et. al [3] who conducted the thermomechanical test on an SMP thin film of polyurethane of the polyester polypol series. The glass transition of the material was 328 K, the thickness of the specimen was about 70 μm. The width was 5 mm, gauge length 25 mm and total length of 75mm.

We will begin the modeling of this material by considering the flow of mechanical power into the system. When a material system is supplied with mechanical power, only a part of it recoverable; the remaining portion of the power that is supplied is dissipated i.e irrecoverably lost. The proportion that is recoverable and that which is dissipated is what gives the material its characteristic behavior or response.
Based on this simple idea, we will develop a model for the material response by relating the recoverable power to changes in the Helmholtz potential and the dissipated power to a rate of dissipation function.

The central feature of this general thermodynamic framework provided by Rajagopal and Srinivasa, 2000, is that the body possesses numerous natural configurations. The response of the material is 'elastic' from these natural configurations, and the rate of dissipation determines how these natural configurations evolve. The viscoelastic response can thus be determined by the Helmholtz potential (ψ) that characterizes the elastic response from the 'natural configuration' and a rate of dissi-

pation function (ξ) that describes the rate of dissipation due to the viscous effects.The way in which the current natural configuration changes is determined by a 'maximum rate of dissipation' criterion subject to the constraint that the difference between the stress power and the rate of change of the stored energy is equal to the rate of dissipation. The dependence of the response function on temperature has far reaching consequences. Polymeric materials near the glass transition show substantial dependence of the elastic modulus on the temperature. This in turn implies through the so-called Maxwell relations, that the entropy of the material will depend on the mechanical variables. This is not an obvious fact and so careful consideration has to be given to modifying purely mechanical models to account for temperature dependence. Ad hoc modifications to the stress response without accounting for the Maxwell relations will lead to internal inconsistencies which will violate the second law of thermodynamics leading to perpetual motion machines. Tobushi [3], in his model, makes such an ad hoc modification leading to inconsistencies in the response function as we will discuss in the following section.

B. Comments on the Response of the SMP Material to be Modeled

As discussed in Chapter I, Tobushi's paper [3] deals with a SMP film undergoing a thermomechanical cycle. The model developed by Tobushi and co-workers, shown in Fig. (17), involved modifying a standard linear viscoelastic model by introducing a slip element due to internal friction. They also took account of the thermal expansion. In order to describe the variation in mechanical properties due to glass transition, coefficients in the model were expressed by a singe exponential function of temperature

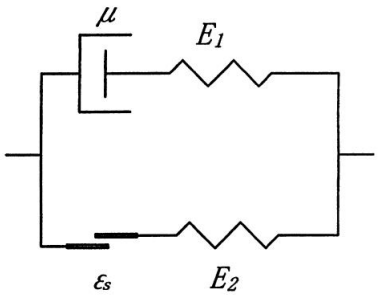

Fig. 17. The mechanical model proposed by Tobushi.

as shown below.

$$\dot{\epsilon} = \frac{\dot{\sigma}}{\hat{E}(\theta)} + \frac{\sigma}{\hat{\mu}(\theta)} - \frac{\epsilon - \epsilon_s}{\lambda} + \alpha\dot{\theta}$$

$$p = p_g exp\{a_p(\frac{T_g}{T} - 1)\}$$

where p is the mechanical property. Even though the dependence of the properties on temperature is stated explicitly above, the rate form of the constitutive equation above does not involve differentiation of the mechanical properties with time. For example, in considering the rate of change of stress σ_1 in the elastic element E_1, the dependence of the elastic modulus on temperature needs to be taken into consideration while differentiating the stress.

$$\sigma_1 = \hat{E_1}(\theta)\epsilon_1$$

$$\dot{\sigma_1} = \hat{E_1}(\theta)\dot{\epsilon_1} + \frac{\partial \hat{E_1}(\theta)}{\partial\theta}\dot{\theta}\epsilon_1$$

Tobushi ignored the second term entirely in his calculations in a similar manner for all temperature dependent parameters while defining the constitutive equation of his model in rate form. There is serious thermodynamical inconsistency in treating the problem this way. It has led to obvious unsatisfactory matches in the model

results and the experimental data as can be seen in Fig. (18).

The stress and strain responses reveal different characteristics in the stress

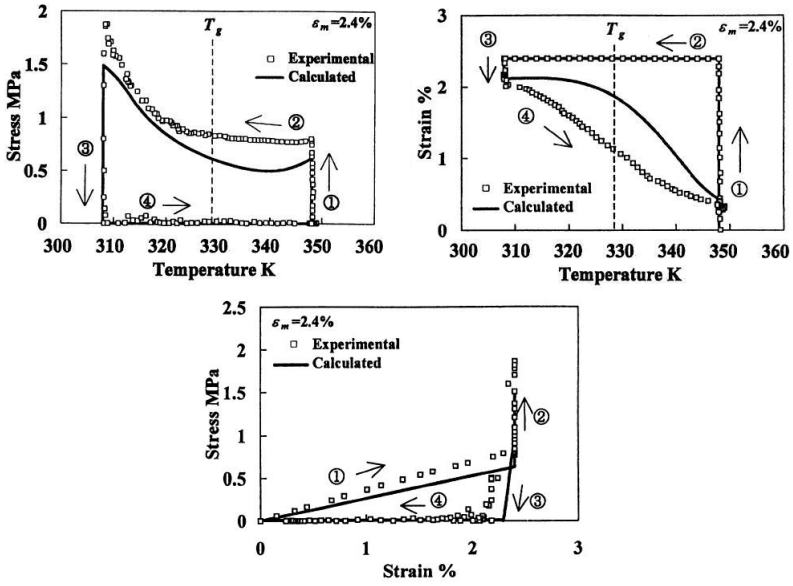

Fig. 18. Experimental and model data from Tobushi's paper.

versus strain graph, and in those versus temperature. However, the thermomechanical cycle also involves strain and stress-relaxing rate, and cooling and heating rates, which is not evident in these graphs. The characteristic trends of stress and strain with respect to time cannot yet be eliminated entirely, since we deal with evolution equations while developing constitutive models for the material. Such behavior, like dependence of the material on history of its response is usually masked in data represented in processed form like above i.e stress versus strain graphs, rather than in desirable raw data form i.e stress versus time and strain versus time.

In the following work, we have extracted information from the above experimental data and re-plotted them against time, which looks like the form shown in Fig.(19). Specifications to this effect are the holding-time during loading and unload-

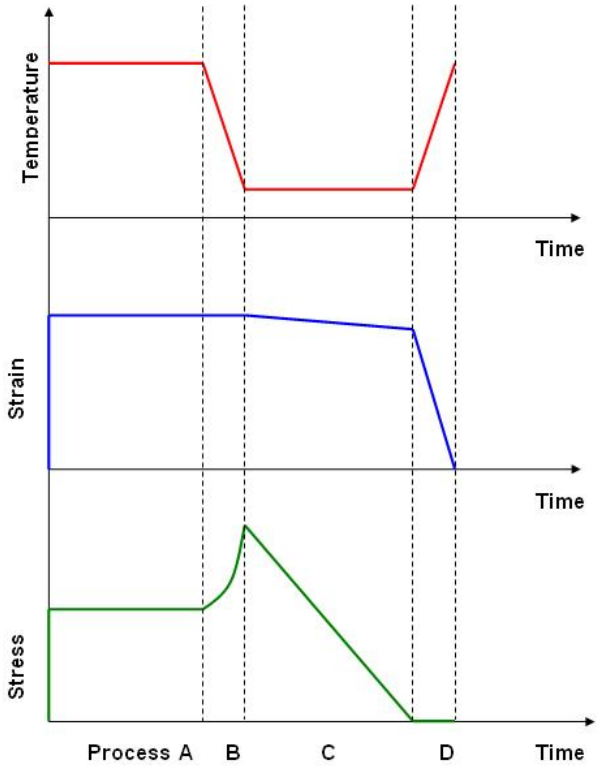

Fig. 19. Experiment under study for the SMP: The processes taking place in a thermomechanical cycle with respect to time.

ing which was 120 minutes, and the heating and cooling rates which were 4K/min. The strain rate was 5 - 50 %.

The model development and simulation shall seek to match the above data in Fig. (18) with respect to temperature and time, and we shall see how some comments on the properties of the material become evident because of this extraction of data in terms of time.

C. Model Philosophy

1. State-evolution Equation Form

Our aim is to systematically obtain the state-evolution equations for the response of the SMP material in the form $\dot{S} = f(S, t)$ where S represents the variables that model the current state of the system and f is a function of the state variables and time.

2. The Power Theorem

Given the external force acting on this system, as well as the temperature control, our task is to find the internal state of the system as a function of time. In order to obtain a thermodynamic approach to the specification of the evolution equations, we consider the input power to the system. Tracking the applied external to the system as it "flows" through the system gives us insight into the mechanisms of storage and dissipation by the system. For any system it is intuitively evident that:

Input Power = Power supplied to the conservative elements + Power dissipated by the dissipative components

Input Power = Rate of change of potential energy of the springs + Power dissipated by the dashpots

This is called the "Power Equation". Since the temperature is changing in this experiment, the potential energy of the system needs to be considered carefully.

For a spring, the work done by it when it goes from one state to another, is equal to the difference in the potential energy between the two states, so that the potential energy difference is also referred to as the isothermal work potential. The Helmholtz potential (or the isothermal work function) of a system is a generalization of this idea: If we change the state of any system from s_1 to s_2 *keeping the temperature* θ *constant*,

then the work supplied to all the conservative components (and hence recoverable) is equal to the difference in the Helmholtz potential. The fact that the Helmholtz potential depends upon the temperature is due to the fact that the spring stiffness may depend upon the temperature. Indeed, for polymers, the modulus can increase or decrease with temperature. Notice that a spring is "repository" of mechanical work so that at times, the power supplied to the spring can be negative, i.e. mechanical power can flow out of the spring. Thus a spring can be both a source as well as a sink of mechanical power.

On the other hand, for the dashpot, the power supplied to any dissipative system cannot be negative, i.e., a dashpot can never be a source of mechanical power, it is always a sink. If we choose evolution equations for dashpots to satisfy this criterion, then we can guarantee that such a material will not become a perpetual motion machine. A viscous dashpot exhibits a velocity dependent force, i.e., the force on a dashpot is a function of the relative velocity of its ends. The equation relating the force on a dashpot to the relative velocity of its ends is called a *kinetic equation*. In the case of a frictional dashpot, one cannot find the velocity v of the dashpot knowing the force on it. The relation for this kind of a dashpot is implicit. All we know is that if the force on the dashpot reaches a critical value, the dashpot "slips" freely. On the other hand, if the force is below the critical level, the velocity of the dashpot is zero and the dashpot "sticks". If, however, the dashpot is connected in series with a spring, then the whole component becomes determinate. This is because, the force is applied to the dashpot indirectly through the spring so that if the dashpot begins to slip freely, the spring slackens and the force on the dashpot drops. On the other hand, if the dashpot sticks, then the spring extends and the force on the dashpot increases so that slip occurs.[27]

The Second Law of thermodynamics implies that during any process, the change

in entropy of the system together with that of its surroundings is non-negative. For our case the amount of entropy η produced by mechanical processes is the power dissipated divided by the temperature,i.e.,

$$d\eta|_{mech,irr} = \frac{\Sigma \sigma_{dashpots} dx_{dashpots}}{\theta} \geq 0$$

Thus, if the dashpot is always made to behave as a sink, then we are ensured of satisfying the Second Law of thermodynamics.

3. The Maximum Rate of Dissipation Criterion

A more conclusive form of the second law is that an isolated system will go to a state of maximum entropy, subject to the external constraints imposed on its state. The power theorem can be written as:

Power Supplied = Rate of recoverable work stored in the system + rate of irrecoverable work lost during the process

This can be derived (as shown in subsequent sections) and we shall lead ourselves to a form of the reduced energy-equation as below:

$$\sigma \dot{\epsilon} = \dot{\psi}|_{\theta} + \xi$$

As discussed in the previous sub-section, the Helmholtz potential ψ represented how much work is recoverable along any given process for the material, and the rate of dissipation ξ described how much work is lost irrevocably along any process. Unlike the Helmholtz potential which is a function of the state, ξ depends upon the process i.e., it is necessarily a function of the path taken by the body in state-space and will be referred to as the dissipation function. Then the allowable processes or paths in state-space are those for which the reduced energy equation is met along the entire

path. There will be many processes that will be allowed from a given state, each with a different amount of work lost. The maximum rate of dissipation hypothesis is as follows: The kinetic equation for any dissipative process is determined by the condition that, among all allowable processes, (subject to the external constraints imposed on the set of possible processes), the actual process proceeds in such a way as to maximize the rate at which mechanical work is dissipated i.e., lost irrecoverably. The maximum rate of dissipation criterion thus suggests that the process followed by the system will be that which produces as much entropy as possible given the constraints.

The cores steps that we are following in the Helmholtz potential approach are thus as follows[27]:

(1) Introducing the Helmholtz potential into the reduced-energy equation

(2) Identifying the elastic parts and dissipative parts of the response

(3) Finding out which variables require kinetic laws and how to state the kinetic laws in such a way as to satisfy the second law of thermodynamics

D. Thermodynamical Considerations

1. Preliminaries

Consider a one-dimensional continuum, i.e a wire, made of shape memory polymer, lying along the X-axis of a co-ordinate system, as shown in Fig. (20). This wire is heated above its glass-transition temperature so that it is in its rubbery state.

Let us label the position of a certain particle in this wire to be X at time $t = 0$. Now, if the wire is elongated, the particle which was at X at time $t = 0$, is now at x at time $t = t$.

The motion of the continuum is given by : $x = \mathbb{F}(X, t)$

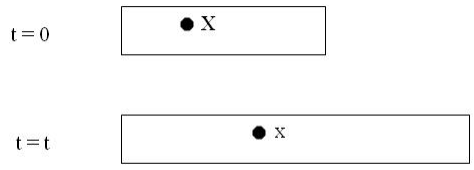

Fig. 20. Particle position in the wire at different time instants.

The deformation gradient of the continuum is given by: $F = \frac{\partial x}{\partial X}$

The velocity gradient of the continuum is given by: $v = \frac{\partial x}{\partial t} = \frac{\partial \mathbb{F}}{\partial t}$

We introduce here the mass density of the wire in the reference configuration to be ρ_r, and in the current configuration to be ρ. For the experiments being conducted on this piece of wire, we denote the axial force being applied on it to be σ.

We start with a minimum set of state variables. Since the experiment we are conducting on the wire involve controlling the stress σ or the strain ϵ as well as the temperature θ of the wire, the minimum set of state variables that can sufficiently describe each particle in the body-set, i.e the wire, are (σ, θ) or (ϵ, θ).

Let the internal energy per unit length be u, the axial heat flux be q and the lateral rate of heat transfer per unit length be r. Body forces are neglected.

The conservation laws are recorded:

We consider a small line element and apply the mass, momentum and energy balance to them, and then by considering the limit as the length of the line element goes to zero, we get the following:

Conservation of Mass:

$$\rho_r = \rho F \tag{3.1}$$

Conservation of Momentum:

$$\begin{aligned} \rho\frac{dv}{dt} &= \frac{d\sigma}{dx} \\ \rho_r\frac{dv}{dt} &= \frac{d\sigma}{dX} \end{aligned} \tag{3.2}$$

Conservation of Energy:

$$\rho\frac{du}{dt} = \sigma\frac{d\epsilon}{dt} - \frac{dq}{dX} + r \tag{3.3}$$

2. The Equation of State

A preliminary list of state variables is given by the density ρ , the internal axial stress σ, the strain ϵ , the internal axial heat flux q, and the temperature θ . Of these, we note that ρ is not an independent state variable since it is directly related to ϵ through Eq.(3.1) . Similarly, the velocity v and the internal energy u do not figure in the independent state variable list since, in principle, they can be computed from the balance laws. We include ϵ_p as one of the state variables for convenience in solving equations as shall be seen when we implement the resulting system equations into MATLAB. Thus the state-variables are given by $S = (\sigma, \epsilon, \epsilon_p, q, \theta)$.

The foundation of the thermodynamical approach presented here is that, the non-dissipative properties of the material are derivable from a single potential, namely the Helmholtz potential for the continuum, while the dissipative properties are explored through the manifestation of the second law of thermodynamics, using the role of the rate of mechanical dissipation as a mechanism for entropy generation.

We commit ourselves to further analysis to be done in the energy-representation

form, where energy is dependent and entropy is the independent variable. The Helmholtz potential being a partial Legendre transform of internal energy, we can write the energy fundamental equation as:

$$u = \hat{u}(\epsilon, \epsilon_p, \eta) \tag{3.4}$$

The corresponding Helmholtz function is:

$$\psi = \hat{\psi}(\epsilon, \epsilon_p, \theta) \tag{3.5}$$

Infact, as explained by Callen [28] from the Legendre transformation of θ as the independent variable, ψ is now given by:

$$\psi = u - \theta\eta \tag{3.6}$$

η now becomes a function of Helmholtz free energy as below:

$$\eta = -\frac{\partial \psi}{\partial \theta} \tag{3.7}$$

Now, we can take the time derivative of the internal energy function in Eq. (3.6):

$$\frac{du}{dt} = \frac{d}{dt}\psi(\epsilon, \hat{\epsilon_p}, \theta) - \frac{\partial \psi}{\partial \theta}\frac{d\theta}{dt} - \theta\frac{d}{dt}\frac{\partial \psi}{\partial \theta} \tag{3.8}$$

Substituting this into the energy conservation equation above in Eq. (3.3):

$$\theta\dot{\eta} = \{\sigma\dot{\epsilon} - (\frac{\partial \psi}{\partial \epsilon}\dot{\epsilon} + \frac{\partial \psi}{\partial \epsilon_p}\dot{\epsilon_p})\} - \frac{dq}{dX} + r \tag{3.9}$$

This is known as the "heat equation" which can be understood from the terms in the equation above as:

Rate of heating = (Rate of heating due to mechanical effects) + axial heat flow + latent heat

The sum that represents the *rate of heating due to mechanical effects* is the one

we are interested in, since it is representative of the thermomechanical coupling. A closer look at this sum shows that the first term represents the mechanical power (or deformation power) supplied to the wire, while the second two terms represent the rate of decrease in recoverable mechanical work. We thus assume that the sum of these terms represent the net mechanical power dissipated by the system. Note that the energy is not lost, but it is unavailable as work. We hence introduce the rate of dissipation ξ through

$$\sigma\dot{\epsilon} - (\frac{\partial\psi}{\partial\epsilon}\dot{\epsilon} + \frac{\partial\psi}{\partial\epsilon_p}\dot{\epsilon_p}) := \xi \tag{3.10}$$

where $\xi \geq 0$

$\therefore$ *Supply of mechanical power - Rate of recoverable mechanical work = Net mechanical power dissipated*

The above identity is referred to as the dissipation relation or the reduced energy relation. The assumption that ξ is non-negative will allow us to satisfy the second law of thermodynamics. This identity can also be equated in the following manner, which represents the reduced energy-rate of dissipation relation for the system at a particular temperature:

$$\sigma\dot{\epsilon} - (\dot{\psi}|_{\theta fixed}) = \xi \tag{3.11}$$

3. Thermomechanical Development of the Model

In the following one-dimensional analysis of the shape memory behavior of an isotropic viscoelastic material, the network of elements are treated such that the material is practically continuous and homogeneous in structure. The model as proposed in the previous chapter is shown in Fig. (21).

In the figure, E_1 and E_2 denote the modulus of the two springs, μ is the viscosity of the viscous dashpot, and k is the viscosity of the friction dashpot. Note that since

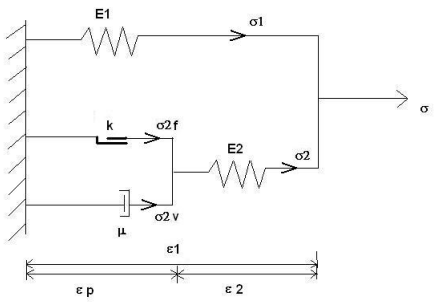

Fig. 21. The proposed mechanical model for the SMP.

the state variables are strain and temperature, these material properties will depend on temperature. The total strain, as already dealt with in the derivations above, is given by ϵ. This strain ofcourse represents the total strain of the material as measured during the experiments, which includes the mechanical strain and the thermal strain of the material. Since we are dealing with a spring-dashpot system, it is capable of representing only the mechanical strain. ϵ_1 shown in the figure is only the mechanical strain. To this we shall have to add the thermal strain of the material so that we now have the total strain of the material. Thus, taking α to be the thermal conductivity of the material, the total strain is given as:

$$\epsilon = \epsilon_1 \tag{3.12}$$

$$\epsilon_2 = \epsilon - \epsilon_p - \alpha\theta$$

The axial pull is σ as indicated in the figure. ϵ_p is the strain of the dampers in parallel, while ϵ_2 is the strain of the spring.

The upper network in the model, as discussed in the previous chapter, represents the rubbery response of the material, which is non-dissipative. The lower network represents the glassy response, which is the dissipative one. Accordingly we will

assume that the stress σ_1 is associated with the rubbery response whereas, stress σ_2 is due to the glassy response. The dashpot is a frictional dashpot that is temperature sensitive. Below the glass transition, the frictional dashpot locks, and prevents the rubbery network from deforming further, leading to a "locked in" strain. On the other hand, at high temperature, the dashpot ceases to operate i.e., its resistance vanishes, and the material behaves like an elastic rubber.

We now proceed with a thermomechanical analysis of this model:

The reduced energy equation for this model is thus given as:

$$\sigma\dot{\epsilon} - (\frac{\partial\psi}{\partial\epsilon}\dot{\epsilon} + \frac{\partial\psi}{\partial\epsilon_p}\dot{\epsilon_p}) := \xi \tag{3.13}$$

Since the state variables are $(\epsilon, \epsilon_p, \theta)$, the stored energy function ψ function depends on $(\epsilon, \epsilon_p, \theta)$ as stated previously. Since the only elements in this model capable of storing energy are the springs, the energy storage function can be explicitly written as:

$$\begin{aligned}\psi &= \frac{1}{2}\hat{E_1}(\theta){\epsilon_1}^2 + \frac{1}{2}\hat{E_2}(\theta){\epsilon_2}^2 \\ &= \frac{1}{2}\hat{E_1}(\theta)(\epsilon)^2 + \frac{1}{2}\hat{E_2}(\theta)(\epsilon - \epsilon_p - \alpha\theta)^2\end{aligned} \tag{3.14}$$

The dissipation will also be a function of the state variables $(\epsilon, \epsilon_p, \theta)$. Hence the rate of dissipation ξ will be a function of $(\dot{\epsilon}, \dot{\epsilon_p}, \dot{\theta})$. The only elements in the model that are capable of dissipating energy are the viscous and friction dampers. Hence the rate of dissipation function will depend on how the viscous damper and the friction damper dissipate energy as indicated below:

$$\xi = \hat{\mu}(\theta)\dot{\epsilon_p}^2 + \hat{k}(\theta)|\dot{\epsilon_p}| \tag{3.15}$$

It is obvious from this equation that ξ depends on $(\dot{\epsilon_p}, \theta)$ only. Later, when we carry out the maximization of the rate of dissipation, it shall involve figuring which state of $(\dot{\epsilon}, \dot{\epsilon_p}, \dot{\theta})$ will give maximum ξ. So, even though ξ depends on $(\dot{\epsilon_p}, \theta)$, we shall be concerned with maximizing only with respect to $(\dot{\epsilon}, \dot{\epsilon_p}, \dot{\theta})$. Since ξ does not depend on $(\dot{\epsilon}, \dot{\theta})$ as seen in Eq. (3.15), we shall maximize only for $(\dot{\epsilon_p})$. Thus for our purpose, ξ is dependent on $(\dot{\epsilon_p})$ alone.

Differentiating Eq. (3.14) with respect to time we obtain:

$$\dot{\psi} = \frac{\partial \psi}{\partial \epsilon}\dot{\epsilon} + \frac{\partial \psi}{\partial \epsilon_p}\dot{\epsilon}_p + \frac{\partial \psi}{\partial \theta}\dot{\theta} \tag{3.16}$$

$$\frac{\partial \psi}{\partial \epsilon} = \hat{E}_1(\theta)(\epsilon) + \hat{E}_2(\theta)(\epsilon - \epsilon_p - \alpha\theta) \tag{3.17}$$

$$\frac{\partial \psi}{\partial \epsilon_p} = -\hat{E}_2(\theta)(\epsilon - \epsilon_p - \alpha\theta) \tag{3.18}$$

Inserting Eq. (3.17) and (3.18), as well as the rate of dissipation function in Eq.(3.15) in the reduced energy relation in Eq. (3.13)

$$\sigma.\dot{\epsilon} - (\hat{E}_1(\theta)(\epsilon) + \hat{E}_2(\theta)(\epsilon - \epsilon_p - \alpha\theta))\dot{\epsilon} + \hat{E}_2(\theta)(\epsilon - \epsilon_p - \alpha\theta)\dot{\epsilon}_p = \hat{\xi}(\dot{\epsilon_p}) \tag{3.19}$$

As discussed above, the rubbery response is non-dissipative. Hence, we expect that the terms involving σ_1 (the rubbery network) will not appear in the rate of dissipation equation. Motivated by the fact that the last term on the left-hand side and the term on the right-hand side of the above equation are the only two terms containing $\dot{\epsilon}_p$, we now stipulate that

$$\begin{aligned} \sigma &= \hat{E}_1(\theta)(\epsilon) + \hat{E}_2(\theta)(\epsilon - \epsilon_p - \alpha\theta) \\ &= \hat{E}_1(\theta)\epsilon - \hat{E}_2(\theta)(\epsilon - \epsilon_p) - \hat{E}_2(\theta)\alpha\theta \end{aligned} \tag{3.20}$$

This is the first constitutive equation of the material. The terms are easy to identify: The first term term is the elastic response of the rubbery network, the second term is the elastic response of the glassy network and the third is the thermal response of the whole network.

Also, for the spring in the glassy network, we note that since the temporary networks in the polymer chains continually break and reform in new configurations, there is considerable dissipation, as explained in the previous chapter. Thus, in the light of the Eq. (3.20), Eq. (3.19) reduces to

$$\hat{\xi}(\dot{\epsilon_p}) = \hat{E_2}(\theta)(\epsilon - \epsilon_p - \alpha\theta)\dot{\epsilon}_p \tag{3.21}$$

Using the stress function in Eq. (3.20), the above equation can be reduced further as below, and this is used as the constraint for the system

$$\hat{\xi}(\dot{\epsilon_p}) = (\sigma - \hat{E_1}(\theta)\epsilon)\dot{\epsilon}_p \tag{3.22}$$

We are thus led to the development of a kinetic equation for ϵ_p which will satisfy the above equation. Now $\xi = \hat{\xi}(\dot{\epsilon_p})$. The actual value of $\dot{\epsilon_p}$ is that which maximizes ξ. Hence by using the standard method of calculus of constrained maximization as explained in Segel [29], we extremize ξ subject to the constraint Eq. (3.22) as follows:

The procedure to extremize a function $f(x)$ subject to constraint $g(x)$ is to find at what x will $\frac{\partial F}{\partial x} = 0$ for

$$F(x, \lambda) = f(x) - \lambda g(x)$$

λ is the Lagrange multiplier whose value is obtained by the satisfaction of the constraint function.

In our model, these will translate as:

$x = \dot{\epsilon_p}$

function f(x) $\Rightarrow \xi = \hat{\xi}(\dot{\epsilon_p})$

constraint g(x) $\Rightarrow \xi - (\sigma - \hat{E_1}(\theta)(\epsilon)\dot{\epsilon_p}) = 0$

F(x,λ) $\Rightarrow \xi - \lambda(\xi - (\sigma - \hat{E_1}(\theta)(\epsilon))\dot{\epsilon_p})$

Thus $\frac{\partial F}{\partial \dot{\epsilon_p}} = 0$ will result as follows:

$$\frac{\partial \xi}{\partial \dot{\epsilon_p}} - \lambda(\frac{\partial \xi}{\partial \dot{\epsilon_p}} - \frac{\partial}{\partial \dot{\epsilon_p}}((\sigma - E_1(\epsilon))\dot{\epsilon_p}) = 0 \tag{3.23}$$

and $\frac{\partial F}{\partial \lambda} = 0$ will result as follows

$$\xi - (\sigma - E_1(\epsilon))\dot{\epsilon_p} = 0 \tag{3.24}$$

Proceeding to solve the maximization problem of Eq. (3.23) and Eq. (3.24)

Differentiating Eq. (3.15) with respect to $\dot{\epsilon_p}$:

$$\frac{\partial \xi}{\partial \dot{\epsilon_p}} = 2\mu\dot{\epsilon_p} + k(sgn(\dot{\epsilon_p})) \tag{3.25}$$

Using this in Eq. (3.23), the Lagrange multiplier can be deduced as follows:

$$(2\mu\dot{\epsilon_p} + k(sgn(\dot{\epsilon_p}))) - \lambda((2\mu\dot{\epsilon_p} + k(sgn(\dot{\epsilon_p}))) - \sigma + E_1(\epsilon)) = 0 \tag{3.26}$$

$$\lambda = \frac{2\mu\dot{\epsilon_p} + k(sgn(\dot{\epsilon_p}))}{2\mu\dot{\epsilon_p} + k(sgn(\dot{\epsilon_p})) - \sigma + E_1(\epsilon)} \tag{3.27}$$

Similarly, using Eq. (3.15) in Eq. (3.24):

$$\mu\dot{\epsilon}_p^2 + k|\dot{\epsilon_p}| - (\sigma - E_1(\epsilon))\dot{\epsilon_p} = 0 \tag{3.28}$$

Thus the values of $\dot{\epsilon_p}$ that maximize ξ are the possible answers of above equation:

$$\dot{\epsilon_p} = 0 \tag{3.29}$$
$$\dot{\epsilon_p} = \frac{\sigma - E_1(\epsilon) - k(sgn(\dot{\epsilon_p}))}{\mu}$$

This leads us to the second constitutive equation of the model, also to be known as the kinetic equation of the system. The dissipative response of the temporary network is described by means of this kinetic equation that shows how the stress in the secondary network gives rise to a gradual change in the temporary nodes leading to a change in the amount by which the temporary network is stretched. As can be seen from the model figure, the change in amount of stretch of the temporary spring, is related to the rate of change of ϵ_2 and this in turn is determined by the nature of the frictional dashpot.

Based on the need for providing both a threshold dry frictional behavior as well as rate dependent subsequent behavior beyond the threshold, we use the above values of $\dot{\epsilon}_p$ and come up with the following criterion:
As discussed at the end of Section (C.2), the Second law of thermodynamics requires

$$\xi = \mu\dot{\epsilon}_p^2 + k|\dot{\epsilon_p}| \geq 0 \tag{3.30}$$

As seen above, in Eq. (3.21),
$\hat{\xi}(\dot{\epsilon_p}) = \hat{E}_2(\theta)(\epsilon - \epsilon_p - \alpha\theta)\dot{\epsilon}_p$
where, $\hat{E}_2(\theta)(\epsilon - \epsilon_p - \alpha\theta) = \sigma_2$

Thus,

$$\sigma_2\dot{\epsilon}_p \geq 0 \tag{3.31}$$

where $\sigma_2 = \mu\dot{\epsilon}_p + k(sgn(\dot{\epsilon_p}))$ from Eq. (3.30)

Thus the signs of σ_2 and $\dot{\epsilon}_p$ should always be the same to satisfy the inequality. The value of $\dot{\epsilon}_p$ depends on the value of σ_2 in comparison with the yield-stress of the friction-damper.

The cases that arise for this comparison are listed as follows:

Case 1:

$$|\sigma_2| < |\hat{k}(\theta)| \tag{3.32}$$

$$\mu\dot{\epsilon_p^2} + \hat{k}(\theta)|\dot{\epsilon_p}| < \hat{k}(\theta)|\dot{\epsilon_p}|$$

The only value of $\dot{\epsilon_p}$ that will satisfy this equation is

$$\dot{\epsilon_p} = 0 \tag{3.33}$$

Case 2:

$$|\sigma_2| > \hat{k}(\theta)$$

This can be analyzed as two sub-cases:

Case 2(a):

$$\sigma_2 > \hat{k}(\theta) \tag{3.34}$$

For this case σ has positive values and hence $sgn(\dot{\epsilon_p})$ is also positive. For this, once again, $\dot{\epsilon_p} = 0$ will satisfy the above inequality, as will $\dot{\epsilon_p} = \frac{1}{\hat{\mu}(\theta)}(\sigma_2 - \hat{k}(\theta))$. However, the former value will give zero rate of dissipation. The value of $\dot{\epsilon_p}$ that will give the maximum rate of dissipation is the latter. Hence this is chosen as the value of $\dot{\epsilon_p}$ as per the maximum rate of dissipation criterion.

Case 2(b):

$$\sigma_2 < -\hat{k}(\theta) \tag{3.35}$$

For this case σ has negative values and hence $sgn(\dot{\epsilon_p})$ is also negative. For this, once again, $\dot{\epsilon_p} = 0$ will satisfy the above inequality, as will $\dot{\epsilon_p} = \frac{1}{\hat{\mu}(\theta)}(\sigma_2 + \hat{k}(\theta))$. However, the former value will give zero rate of dissipation. The value of $\dot{\epsilon_p}$ that will give the maximum rate of dissipation is the latter. Hence this is chosen as the value

of $\dot{\epsilon_p}$ as per the maximum rate of dissipation criterion.

Thus, we can write these three threshold conditions as the viscoplastic equation of the model:

$$\dot{\epsilon_p} = \begin{cases} 0, & |(\sigma - \hat{E_1}(\theta)(\epsilon))| \leqslant \hat{k}(\theta); \\ \frac{1}{\hat{\mu}(\theta)}(\sigma - \hat{E_1}(\theta)(\epsilon) - \hat{k}(\theta)), & (\sigma - \hat{E_1}(\theta)(\epsilon)) > \hat{k}(\theta); \\ \frac{1}{\hat{\mu}(\theta)}(\sigma - \hat{E_1}(\theta)(\epsilon) + \hat{k}(\theta)), & (\sigma - \hat{E_1}(\theta)(\epsilon)) < -\hat{k}(\theta) \end{cases} \tag{3.36}$$

The above set of cases can be written in a compact form as

$$\dot{\epsilon_p} = \frac{1}{\hat{\mu}(\theta)}\{\langle \sigma - E_1(\epsilon) - \hat{k}(\theta)\rangle - \langle -\hat{k}(\theta) - \sigma + E_1(\epsilon)\rangle\} \tag{3.37}$$

where $\langle x \rangle = \frac{1}{2}(x + \|x\|)$.

A schematic plot of $\dot{\epsilon_p}$ versus σ_2 is shown in Fig. (22). Note that the stress on

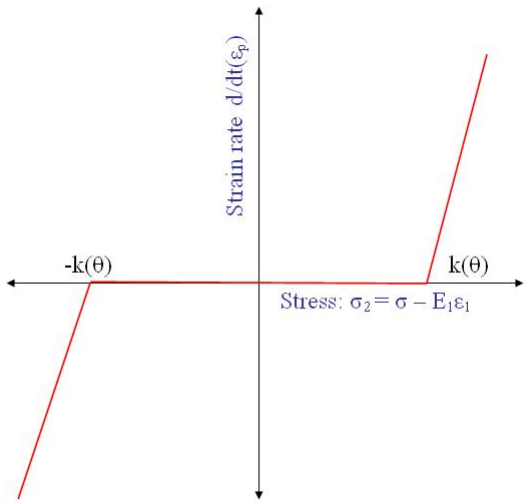

Fig. 22. Schematic figure representing response of the frictional dashpot.

the dashpot is σ_2 (plotted along the x-axis) while the strain rate associated with it is $\dot{\epsilon_p}$ (plotted along the y-axis). Until the driving force σ_2 exceeds $\hat{k}(\theta)$, the dashpot

locks, i.e $\dot{\epsilon_p} = 0$. Beyond that, the dashpot is assumed to be linear with a slope μ . Of course, we shall consider non-linear viscous behavior where this slope will change as $\mu(\theta)$, that reflects the response more accurately. Qualitatively, the "locking" of the dashpot if the magnitude of the driving force σ_2 is less than $\hat{k}(\theta)$, is the origin of shape fixity in this model.

The state of the material is represented by the variables $S = (\sigma, \epsilon, \epsilon_p, q, \theta)$. Equations (3.20) and (3.36) represent two constitutive equations for the response of the material. Remaining three equations needed to solve for this five-variable system can be specified in the control equation of stress/strain input, the input function of the temperature θ, and lastly the equation of momentum conservation Eq. (3.2) combined with the the heat-equation Eq. (3.9), which shall talk of the variable q. In the latter equation, we will specify the axial conduction and the lateral heating through:

$$q = -\alpha \frac{d\theta}{dX} \tag{3.38}$$

$$r = -h(\theta - \theta_\infty) \tag{3.39}$$

where α and h are the thermal conductivity and lateral heat transfer coefficients and θ_∞ is the temperature of the ambient atmosphere. For a straight wire in equilibrium, the momentum conservation and heat-equation reduces to:

$$\frac{d\sigma}{dX} = 0 \Rightarrow \sigma = constant \tag{3.40}$$

$$-\theta \frac{d}{dt}\frac{\partial \psi}{\partial \theta} = \xi - k\frac{d^2\theta}{dX^2} - h(\theta - \theta_\infty) \tag{3.41}$$

The equations simplify further if we assume that the temperature is uniform so that there is no axial heat flux, i.e $\frac{d\theta}{dX} = 0$. In this case, the above heat-equation also simplifies into an ODE of the following form, on substitution of ξ:

$$-\theta \frac{d}{dt}\frac{\partial \psi}{\partial \theta} = \sigma_2 \dot{\epsilon_p} - h(\theta - \theta_\infty) \tag{3.42}$$

This last assumption regarding the uniformity of the temperature is problematic and should considered carefully since these polymers are generally poor heat conductors and so local high temperatures can persist for substantial periods of time. However, in the interests of a *simplistic* model leading to a collection of ordinary differential equations, we will ignore this technologically significant issue and simply assume that the heating cooling and deformations are done so slowly that there is no axial temperature gradient. Thus the number of variables reduces to four: $\mathbb{S} = (\sigma, \epsilon, \epsilon_p, \theta)$. We shall now proceed to show the implementation of the system equations derived, in MATLAB, and simulate the experimental results extracted from Tobushi's paper.

CHAPTER IV

SIMULATION

To doubt everything, or, to believe everything, are two equally convenient solutions; both dispense with the necessity of reflection - Jules Henri Poincaré

A. Implementation of the System Equations into Matlab

We view the SMP as a dynamical system i.e., one whose state changes are given by a suitable differential equation. As discussed in section C.1 in the previous chapter, we have obtained the system of model equations for the material in state evolution form. This will translate as below to suit our purpose of implementing the equations in MATLAB:

$$\dot{S} = f(S, t) \tag{4.1}$$

where S represents the variables that model the current state of the system and f is a function of the state variables and time.

The state of the material is represented by the variables $S = (\sigma, \epsilon, \epsilon_p, \theta)$. As seen Eqns. (3.20) and (3.36) represent two constitutive equations for the response of the material. Remaining two equations needed to solve for this system are specified in the control equation of stress /strain input and the input function of the temperature. The problem with the implementation of these equations is that some of them are in algebraic form whereas others are in rate form. Given the ease with which computer program MATLAB is able to deal with differential equations, and in view of their versatility, we will write all the equations in rate form.

The set of equations below represents, in concise form, four differential equations for the four state variables $S = (\sigma, \epsilon, \epsilon_p, \theta)$. A few comments are in order with regard

to this set of differential equations.

Force or Strain Control:

$$A(t)\dot{\sigma} + B(t)\dot{\epsilon} = g(t) \tag{4.2}$$

This is a single differential equation with time dependent coefficients for force or strain control. This is a very concise way to deal with complicated specifications. We simply set A or B to zero in the appropriate time interval when either strain or stress is specified.

State Equation:

Eq.(3.20) can be rewritten in rate form as follows:

$$\dot{\sigma} - E_1\dot{\epsilon} - E_2(\dot{\epsilon} - \dot{\epsilon_p}) + \alpha(E_2)\dot{\theta} - \{\frac{dE_1}{d\theta}\epsilon + \frac{dE_2}{d\theta}(\epsilon - \epsilon_p) - (\frac{dE_2}{d\theta})\alpha\theta\}\dot{\theta} = 0 \tag{4.3}$$

We can identify the terms that appear in the equation in a straight forward manner. The second and third terms are the elastic stress rate of the glassy network and rubbery network respectively, the fourth term is the thermal stress rate. However, the last term is due to changes in moduli with temperature and does not have a specific name as such. From a thermodynamical point of view, if the moduli depend upon the temperature, these terms cannot be ignored (while retaining the temperature dependence of the moduli) since otherwise the results will be inconsistent.

Kinetic Equation:

$$\dot{\epsilon_p} = \begin{cases} 0, & \left|\left|(\sigma - \hat{E_1}(\theta)(\epsilon))\right|\right| \leqslant \hat{k}(\theta); \\ \frac{1}{\hat{\mu}(\theta)}(\sigma - \hat{E_1}(\theta)(\epsilon) - \hat{k}(\theta)), & (\sigma - \hat{E_1}(\theta)(\epsilon)) > \hat{k}(\theta); \\ \frac{1}{\hat{\mu}(\theta)}(\sigma - \hat{E_1}(\theta)(\epsilon) + \hat{k}(\theta)), & (\sigma - \hat{E_1}(\theta)(\epsilon)) < -\hat{k}(\theta) \end{cases} \tag{4.4}$$

In the Helmholtz potential approach presented here, ϵ_p is a defined variable and NOT a primitive, it can be completely eliminated by simply substituting Eq. (4.10) into Eq. (4.9) and removing ϵ_p from the list of state variables. It is however convenient

to keep this variable in the list since it considerably simplifies the understanding of the shape memory effect and represents a lower bound to the strain that can be retained at any instant. In other words, the value of ϵ_p will tell us what is the minimum strain that can be retained at any given state, so that, by monitoring its value during a process, we will be able to estimate whether the target shape retention has been reached or exceeded.

Temperature Specification:

$$\dot{\theta} = f(t) \tag{4.5}$$

This is the input equation. If one desires to model a process where the temperature of the wire is not known, but only the ambient temperatures is known, then one needs to replace Eq. (4.11) with the heat equation Eq. (3.42).

B. Simulation of the SMP Response

1. Simulation Specifications of the Thermomechanical Cycle

Since we are dealing with rate equations to describe the system, we have extracted the experimental data from Tobushi's work with respect to time. For this the specifications of the processes are [3]:

a. The strain-rate was 5-50% per minute.

b. Each loading and unloading hold-time was 120 minutes.

c. The heating-cooling rate was 4K per minute.

d. Total rise or drop in temperature was 40K.

In order to simulate the thermomechanical process, we will use the set of differential equations (4.8) to (4.11). The thermomechanical process is as follows:

1. *Initial conditions:* The material is assumed to be in a stress free state at a tem-

perature above the glass transition temperature $\theta_g = \theta_g + 20$. All strains are to be measured from this state.

2. *Process A: High temperature stretching*: We assume that the temperature is held fixed at θ_{max} and the strain is increased steadily at a prescribed rate g_1 for a time $0 < t < t_1$. Thus $f(t) = 0, A(t) = 0, B(t) = 1, g(t) = g_1$ for this time interval.

3. *Process B:Fixing the temporary shape*: The strain is fixed at g_1 and the temperature is lowered to $\theta_{min} = \theta_g - 20$ at a predetermined rate a. During this process, due to fact that thermal contraction processes are not allowed to take place, the stress rises to σ_{max}. Thus for $t_1 < t < t_2, (t_2 = 40/a)$ we have $f(t) = a, A(t) = 0, B(t) = 1, g(t) = 0$; the last condition guarantees that the strain is fixed during this time interval.

4. *Process C: Relaxing the stress*: Now the temperature is fixed at θ_{min} and the stress is gradually relaxed to zero at a predetermined rate $b < 0$. During this process, a permanent strain sets in. Thus for $t_2 < t < t_3, (t_3 = t_2 - \sigma_{max}/b)$, we have we have $f(t) = 0, A(t) = 1, B(t) = 0, g(t) = b$; the last condition guarantees that the strain is fixed during this time interval. The material has now attained its temporary shape.

5. *Process: D Recovering the original shape*: Now the body is heated at a rate a in a stress-free state back to the original temperature to recover the original shape. Thus for $t_3 < t < t_4$ we have $f(t) = -a, A(t) = 1, B(t) = 0, g(t) = 0$. The strain slowly relaxes.

2. Temperature Dependence Form of Material Parameters

The key to the response of the SMP material is the temperature dependence of the mechanical properties. We will assume very simple forms for the parameters of this model essentially assuming that the temperature dependence of them is a sigmoidal shape that asymptotes from a low value at high temperature h_{high} above the glass transition temperature to a different high value at low temperature h_{low}. In order to illustrate the response of the material, we first introduce a function of the temperature θ that is akin to a smoothed step function and represents a smooth transition from zero to one as the temperature ranges from below θ_g to above θ_g, this function is of the form:

$$h(x, x_t) = \begin{cases} 0, & x < -x_t; \\ sinh(x - constant)) & -x_t < x < x_t; \\ 1, & x > x_t \end{cases} \tag{4.6}$$

We will use this function to introduce the temperature dependence of the material parameters in this problem. Of course, this assumption is not validated by any statistical or structure-property relationship from polymer science. However,this is a very simple assumption that requires only one parameter the transition value x_t in order to represent the change in properties. The transition value in our case will be $\theta \pm 20$.

Suppose p is the mechanical property, then the property will have the following trend:

$$p = p_{\theta_{max}} + (p_{\theta_{max}} - p_{\theta_{min}}) \times h(\theta, \theta_g \pm 20) \tag{4.7}$$

The temperature dependence of the mechanical properties of the material, may not have necessarily the above form. We shall explore other forms of dependence to simulate the behavior of the SMP. But we wish to emphasize that the gross features

of the response can be imitated by a change in property with temperature. Attention to finer details of the response will bring to light, the forms of the properties and their dependent variables. We now proceed to non-dimensionalize the equations of the system.

C. Non-dimensionalization of the System Equations

In order to systematically non-dimensionalize all the variables, we note that the strains in most of the experimental papers are around 2.4% to about 10% and the stresses are of the order of the high-temperature rubbery modulus times the strain.

Thus, we introduce the following non-dimensionalizing variables:

(1) The glass transition temperature θ_g.

(2) The maximum strain applied ϵ_0 from experimental results.

(3) The typical stress response at high temperature and constant applied strain, σ_0 from experimental results.

(4) The non-dimensionalization of the time, since this is connected with the kinetic response.

Thus, we systematically non-dimensionalize static variables as $S = (\overline{\sigma}\sigma_0, \overline{\epsilon}\epsilon_0, \overline{\epsilon_p}\epsilon_0, \overline{\theta}\theta_g)$ and using the non-dimensional time $\bar{t} = t/t_0$ where the over-lined variables are non-dimensional.We note that the term $\sigma_0\epsilon_0$ has the dimensions of energy and thus, we will define a non-dimensional Helmholtz potential as $\overline{\psi} = \psi/(\sigma_0\epsilon_0)$.

Thus the parameters used to non-dimensionalize the equations here are as follows: $C = \sigma_0/\epsilon_0$

$\bar{\gamma} = \alpha\theta_0/\sigma_0$

Hence the non-dimensional quantities can be tabulated as in Table (II).

Table II. Dimensional Quantities and Corresponding Non-dimensional Quantities

Dimensional	Non-dimensional
σ	$\bar{\sigma} = \frac{\sigma}{\sigma_0}$
ϵ	$\bar{\epsilon} = \frac{\epsilon}{\epsilon_0}$
ϵ_p	$\bar{\epsilon_p} = \frac{\epsilon_p}{\epsilon_0}$
t	$\bar{t} = \frac{t}{t_0}$
θ	$\bar{\theta} = \frac{\theta}{\theta_g}$
E_1	$\bar{E_1} = \frac{E_1}{C}$
E_2	$\bar{E_2} = \frac{E_2}{C}$
μ	$\bar{\mu} = \frac{\mu}{t_0 C}$
k	$\bar{k} = \frac{k}{C}$

Besides the above non-dimensional quantities, we take the following values for the parameters enlisted in Table (III), which are decided based on non-dimensionalizing the experimental data from Tobushi's [3] experimental data for $\epsilon_{max} = 2.4\%$, so that comparison of model and experimental data is sensible.

Table III. Parameter Values for Non-Dimensionalization and Their Significance

Parameter	Value	Significance
σ_0	0.7968 Mpa	Experimental value of stress at constant high temperature and maximum applied constant strain
ϵ_0	0.023046	Experimental maximum applied constant strain
θ_g	328 K	Glass-transition temperature of polyurethane sample
t_0	100 sec	Suitable fraction of rate experimental processes
α	$11.6 \times 10^{-5} K^{-1}$	Conductivity of the polyurethane sample (this mechanical property is treated as a constant for the thermomechanical experiment)

D. Non-Dimensional System of Equations

Force or Strain Control:

$$A(\bar{t})\dot{\bar{\sigma}} + B(\bar{t})\dot{\bar{\epsilon}} = g(\bar{t}) \tag{4.8}$$

State Equation:

Eq.(3.20) can be rewritten in rate form as follows:

$$\dot{\bar{\sigma}} - \bar{E}_1\dot{\bar{\epsilon}} - \bar{E}_2(\dot{\bar{\epsilon}} - \dot{\bar{\epsilon_p}}) + \bar{\gamma}(\bar{E}_2)\dot{\bar{\theta}} - \frac{d\bar{E}_1}{d\bar{\theta}}\bar{\epsilon} - \frac{d\bar{E}_2}{d\bar{\theta}}(\bar{\epsilon} - \bar{\epsilon_p}) + (\frac{d\bar{E}_2}{d\bar{\theta}})\bar{\gamma}\bar{\theta}\dot{\bar{\theta}} = 0 \tag{4.9}$$

Kinetic Equation:

$$\dot{\epsilon_p} = \begin{cases} 0, & \left|\left|(\bar{\sigma} - \bar{E}_1(\bar{\epsilon}))\right|\right| \leqslant \bar{k}; \\ \frac{1}{\bar{\mu}}(\bar{\sigma} - \bar{E}_1(\bar{\epsilon}) - \bar{k}), & (\bar{\sigma} - \bar{E}_1(\bar{\epsilon})) > \bar{k}; \\ \frac{1}{\bar{\mu}}(\bar{\sigma} - \bar{E}_1(\bar{\epsilon}) + \bar{k}), & (\bar{\sigma} - \bar{E}_1(\bar{\epsilon})) < -\bar{k} \end{cases} \tag{4.10}$$

Temperature Specification:

$$\dot{\bar{\theta}} = f(t) \tag{4.11}$$

Thus, with these non-dimensional system of equations, we can proceed to feed them into MATLAB in the following form.

$$\begin{bmatrix} A & B & 0 \\ 1 & -(\bar{E}_1 + \bar{E}_2) & \bar{E}_2 \\ 0 & 0 & 1 \end{bmatrix} \begin{bmatrix} \dot{\bar{\sigma}} \\ \dot{\bar{\epsilon}} \\ \dot{\bar{\epsilon_p}} \end{bmatrix} = \begin{bmatrix} g(\bar{t}) \\ -\bar{\gamma}\bar{E}_2\dot{\bar{\theta}} - \frac{\partial\bar{E}_2}{\partial\theta}\bar{\gamma}\bar{\theta}\dot{\bar{\theta}} \\ -\frac{1}{\bar{\mu}}\bar{k}a^3 \end{bmatrix} + \begin{bmatrix} 0 & 0 & 0 \\ 0 & (\frac{\partial\bar{E}_1}{\partial\theta} + \frac{\partial\bar{E}_2}{\partial\theta}) & -\frac{\partial\bar{E}_2}{\partial\theta} \\ \frac{1}{\bar{\mu}}a^2 & -\frac{\bar{E}_1}{\bar{\mu}}a^2 & 0 \end{bmatrix} \begin{bmatrix} \bar{\sigma} \\ \bar{\epsilon} \\ \bar{\epsilon_p} \end{bmatrix} \tag{4.12}$$

where,

$$a = \begin{cases} 0, & \left|\left|(\sigma - \hat{E}_1(\theta)(\epsilon))\right|\right| \leqslant \hat{k}(\theta); \\ 1, & (\sigma - \hat{E}_1(\theta)(\epsilon)) > \hat{k}(\theta); \\ -1, & (\sigma - \hat{E}_1(\theta)(\epsilon)) < -\hat{k}(\theta) \end{cases} \tag{4.13}$$

Thus the equations have been fed in the form $A_{(x,\theta,t)}\dot{x} = p_{(x,\theta,t)} + Q_{(x,\theta,t)}x$, which can be solved by the ODE45 solver in MATLAB in a straight-forward manner.

CHAPTER V

RESULTS

For every fact there is an infinity of hypotheses. Robert M. Pirsig, Zen and the Art of Motorcycle Maintenance, 1974

A. Simulation Results

The entire thermomechanical cycle simulation results for the shape memory polyurethane sample is shown below in Figure (23 a,b,c,d). The four graphs are drawn together so that the reader may get a good idea as to how the processes occur. Fig. (23) shows (a) The full 3-D view of the response. (b) The stress versus temperature response obtained as a projection of the figure (a) along the strain axis (c) The strain versus temperature response obtained as a projection along the stress axis, and (d) the stress-strain response obtained as a projection along the temperature axis. We shall talk about the results by decoupling the four processes of loading, cooling, unloading and heating in the following analysis, and explain the physical implications in the model behavior from these results, thereby gaining an insight about how the material behaves in this thermomechanical cycle. The processes unfurled with respect to time is as shown in Figure (24) below showing (a) The temperature control for the whole cycle. (b) The stress versus time response of the material (c) The strain versus time response, and (d) the plastic-strain response of the dampers in the model.

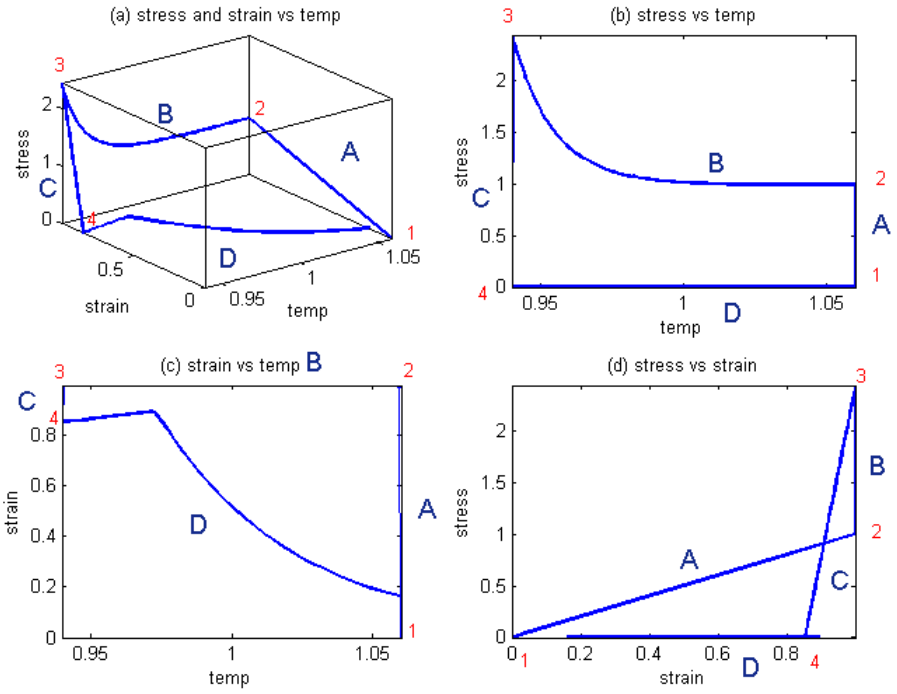

Fig. 23. Simulation of response of SMP to a full thermomechanical cycle.

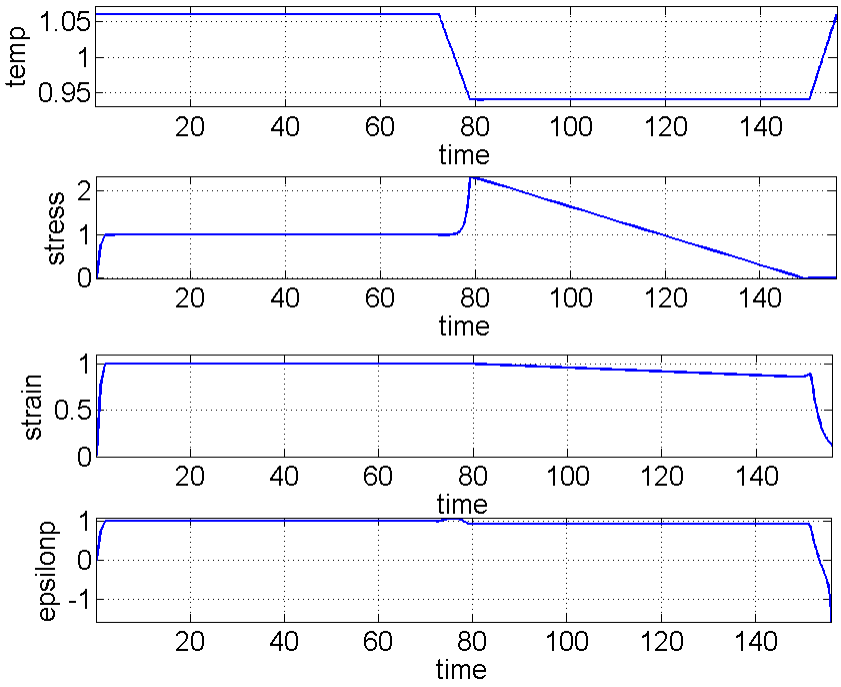

Fig. 24. Simulation of the response of the SMP to a full thermomechanical cycle with respect to time.

B. Explanation of Model Behavior

In qualitative terms, the operation of the model is explained as follows:

1. Initial Conditions

The material is at a temperature that is higher than θ_g in an un-stretched state (refer to point 1 in Figure (23c) above. This is the reference state for the strain measurements and hence all deformations including thermal expansion/contraction will be measured from this high temperature state of the material.

2. Process A: High Temperature Stretching

We stretch the material instantaneously to a strain ϵ_{max} (point 2 in Figure (23c)). Because of the instantaneous strain applied, there is an instantaneous rise in stress in both the networks. The rubbery network elongates like an elastic material. Note that at this temperature the yield-stress $\hat{k}(\theta)$ is set to almost zero. The instantaneous rise in strain causes instantaneous rise in stress in the dampers [22] as well. Within this fraction of time, the instantaneous rise in stress in the dry-friction damper overcomes its yield-stress $\hat{k}(\theta)$ and hence the plastic strain starts rising in the dampers as shown in Figure (25).

After this rise, the stress reaches a constant value, which is a result of both the rubber and the glassy springs, and is sensitive to the high temperature value of the modulus of the rubbery spring. Once the stress reaches a constant value, there is no more sliding of the dry-friction damper, and hence the plastic strain gets "locked-in" after the initial rise. The glassy-spring and the dampers are in series, and hence the spring adjusts to fit the sliding of the damper and the thermal strain (which is zero at this stage) and thus maintains the constant applied strain.

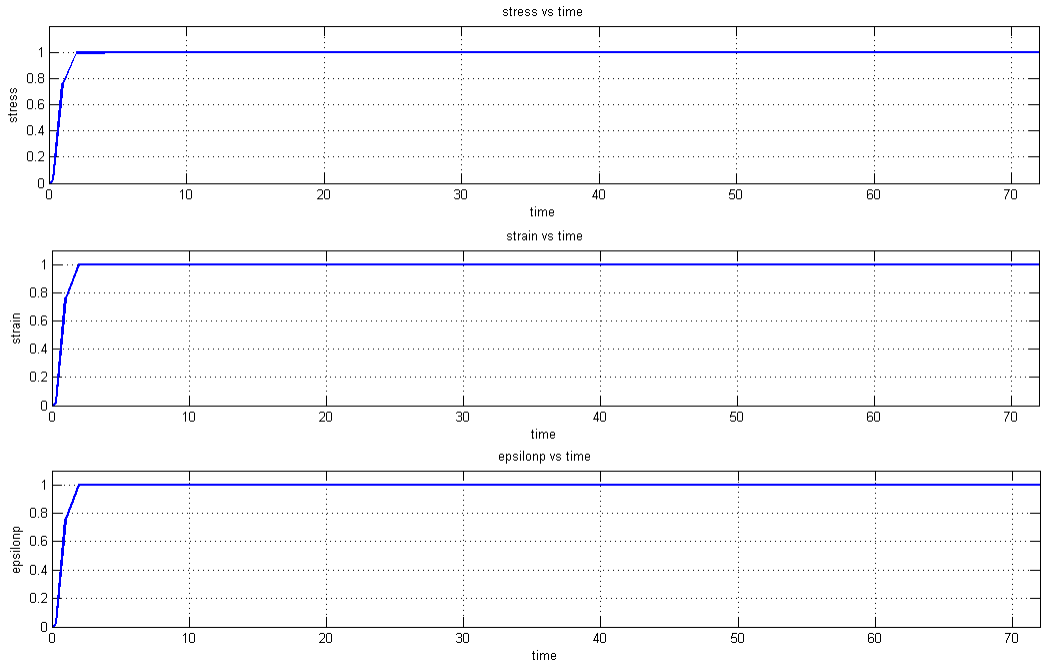

Fig. 25. Stress, strain and plastic strain response of material during Process A of high-temperature stretching.

Physically, as the wire is stretched, as shown in Figure (26) the permanent backbone polymer chains of the material start uncoiling (as accounted for by the elongation of rubbery spring.) Simultaneously, temporary junctions are forming and breaking at a high rate. Very few junctions are able to hold on as the yield-stress of the material at high temperature is very low.

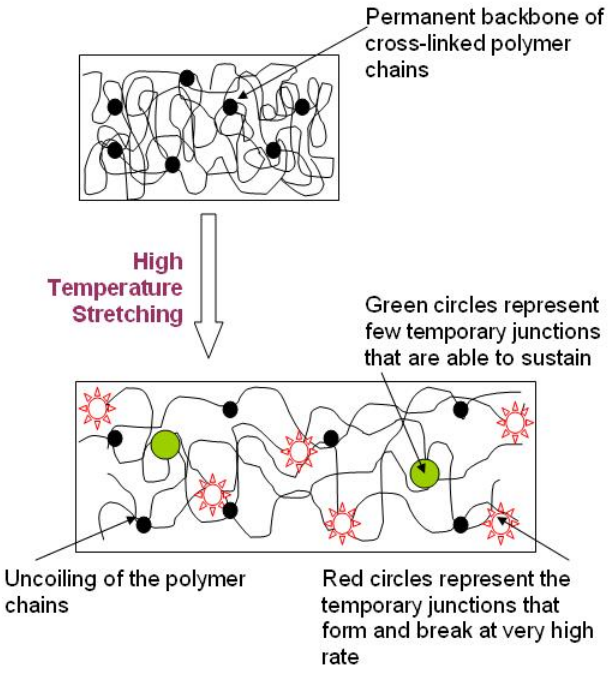

Fig. 26. Process A: Effect of high temperature stretching process in polymer.

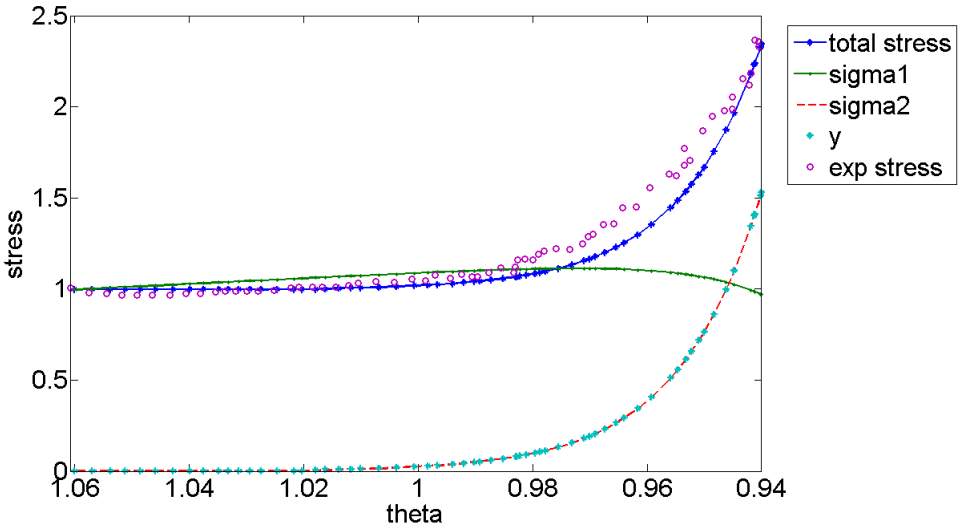

Fig. 27. Trend of stress rise in the material vs temperature during the constant strain cooling process.

3. Process B:Cooling and Fixing the Temporary Shape

The strain is fixed at ϵ_{max} and the temperature is lowered to $\theta_{min} = \theta_g - 20$ at a rate $4K/sec$. The stress developed here in the material has the following trend as shown in the graphs in Figure (27).

The rising trend of stress can be explained on account of three reasons: First, the material is cooled while the total strain of the material is maintained at ϵ_{max}. Because of the tendency of the material to contract under cooling, thermal stresses rise linearly in the material with decrease in temperature. The contraction in the material is barely 0.19% of the total strain. The thermal stress therefore, affects the magnitude of the rise in stress, however its linear rising trend does not contribute much to the stress rise trend in above figure.

Hence we move to the second reason: Since the material tends to contract, mechanical strain applied to the material has to be increased here so that the total

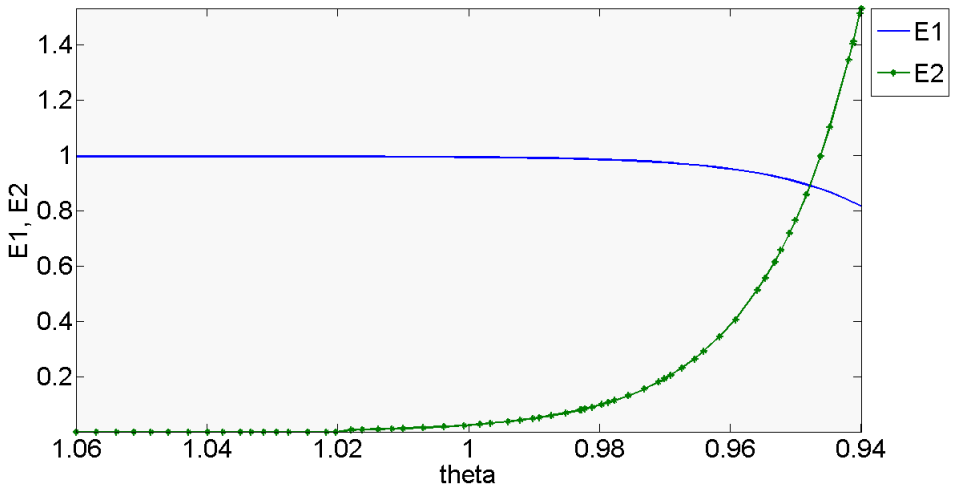

Fig. 28. Trend of modulus in the material vs temperature during the constant strain cooling process.

strain of the material remains at ϵ_{max}. Thus mechanical stresses are induced in the material. The magnitude of stress induced depends directly on the modulus of the material which is changing with temperature as a combination of $\hat{E}_1(\theta)$ and $\hat{E}_2(\theta)$ as shown in Figure (28). Notice carefully, the rise/fall in moduli is not much until θ_g. After θ_g the rise/fall in moduli is evident and is mimicked by the stress rise. However, the rising trend is trade off between the fall in stress in the rubbery network and the rise in stress in the glassy network. Also, the trend of the stress cannot be likened entirely to the trend of the modulus (different functions besides hyperbolic sine used here, i.e. hyperbolic tangent, also give a similar rise in stress), because the stress rate depends not only on the modulus but also on the gradient of the modulus. Thus the rise of stress can be controlled by defining suitable functions of the moduli of the two springs, and specifying the low temperature values of the moduli.

This brings us to the final reason reason why the stress in the glassy network

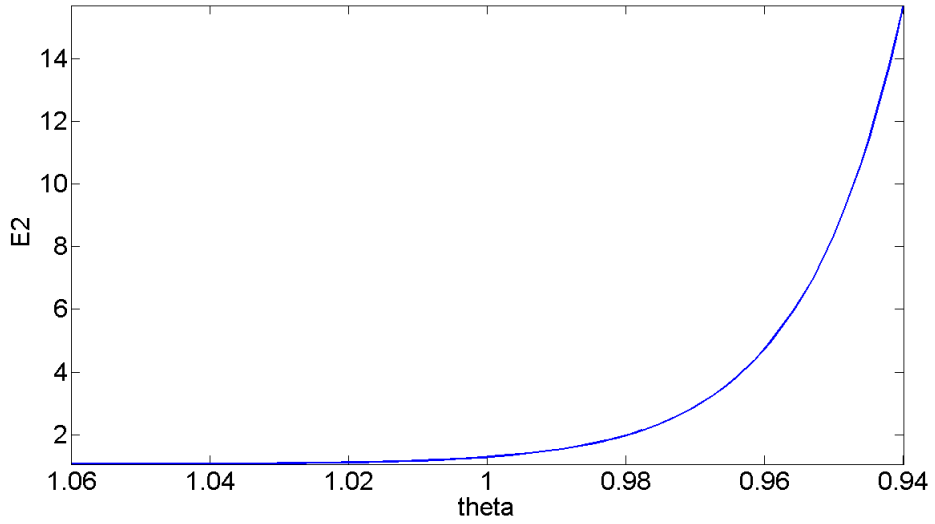

Fig. 29. Rising trend of yield-stress during cooling process.

and the corresponding plastic strain rises in the manner shown above. This is mainly due to the rise in the yield stress of the material. The stress in the glassy network overcomes the yield-stress of the friction damper and hence the damper slips further and accounts for the increase in applied mechanical strain. The yield-stress of the material is prescribed to be almost constant above glass-transition (refer to Figure (29)), and starts rising rapidly only at lower temperatures below glass-transition [30]. Because of this, the rise in stress can be controlled carefully, and kept constant till temperature drops to θ_g, and then the stress is made to rise in desired fashion at lower temperatures.

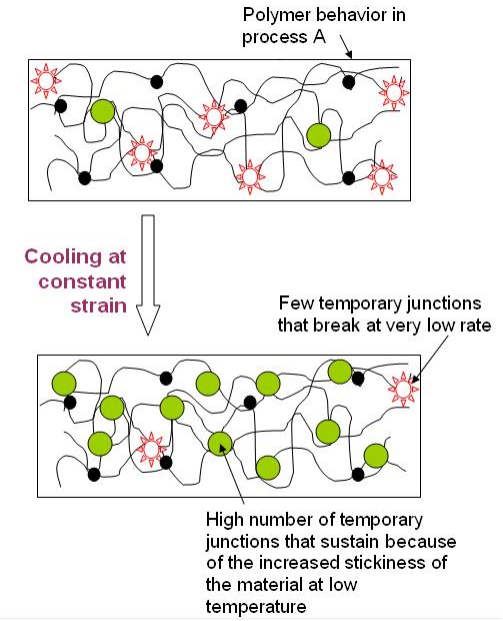

Fig. 30. Process B: Effect of cooling at constant strain in the polymer.

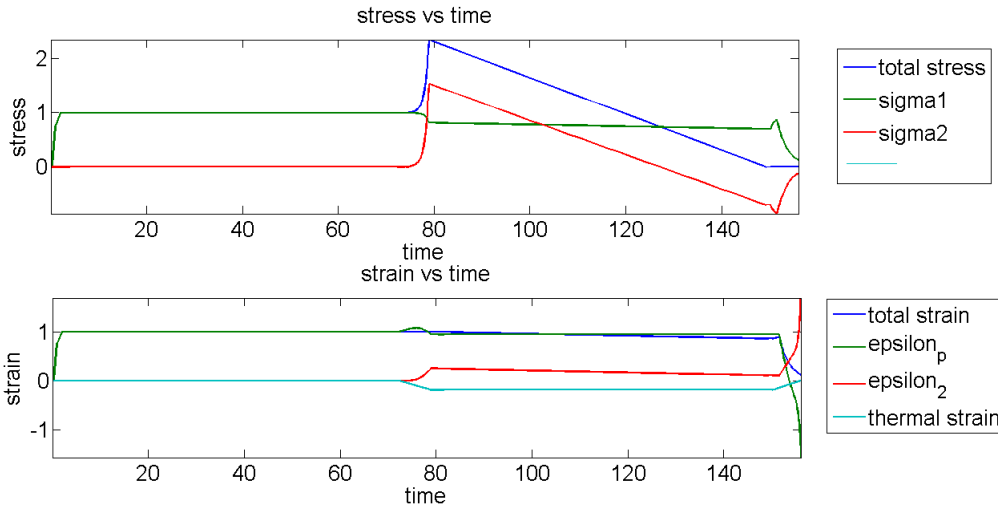

Fig. 31. Stress and strain in various elements of the model during Process C of unloading at low temperature.

Physically, as shown in Figure (30), the permanent backbone of polymer chains remains uncoiled as from previous region. As the temperature is lowered, mobility of the chains decreases. The yield-stress of the material rises in this region, and it increases the stickiness of the material and hence the temporary-junction formation rate is greater than junction breakage rate. Lots of temporary junctions are formed that sustain and this helps material maintain the temporary shape while cooling.

4. Process C: Unloading the Material at Constant Low Temperature

Now, the load is removed at a constant rate, keeping the material at constant low temperature. The yield-stress of the material at the end of the previous process was very high.

Refer to the Figure (31) that shows the stresses in various elements of the model from time instant 79 to 150. The stress in both rubber and glassy network is

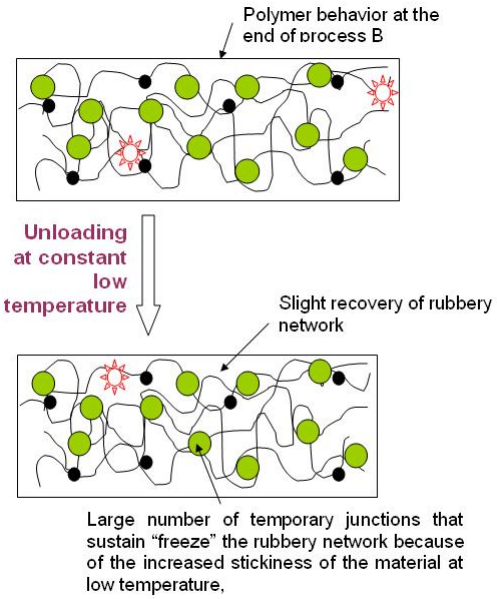

Fig. 32. Process C: Effect of unloading at low temperature in the polymer.

steadily reducing with removal of load, and hence the plastic strain in the material is locked in at the value reached at the end of the previous process. The stress in the rubber network was low to begin with here, as the elastic modulus of the rubbery spring reached a very low value at the end of the process B. This stress remains constant throughout the process of unloading. Hence, the unloading of the stress directly affects only the stress in the temporary(glassy) network. It reduces at the same rate as unloading, and since the modulus of the glassy spring is high here, the spring contracts further. It soon starts compressing the spring around the time instant 130. Thus the stress in this temporary network, even though in compression, its magnitude does not exceed that of the yield-stress and hence the plastic strain is "locked-in" throughout the region.

Since the temperature in this range is not changing, the thermal strain in this

region is constant at the value reached in previous range of thermal contraction. Thus the total strain is the result of the locked-in plastic strain and the contracting elastic strain of the glassy spring. That is why the model shows a slight decrease in strain here which accounts for the shape fixity of the model. To get very less strain recovery here, the glassy spring should be made as stiff as possible.

Physically, as shown in Figure (32), because the yield-stress of the material here is very high, the temporary junctions formed previously, persist in this region, as their threshold for breaking is now very high. The material recovers slightly as the stress is reduced and this allows slight recovery of the permanent rubbery chains. However this recovery is very low because the temporary junctions formed "freeze" the rubbery network.

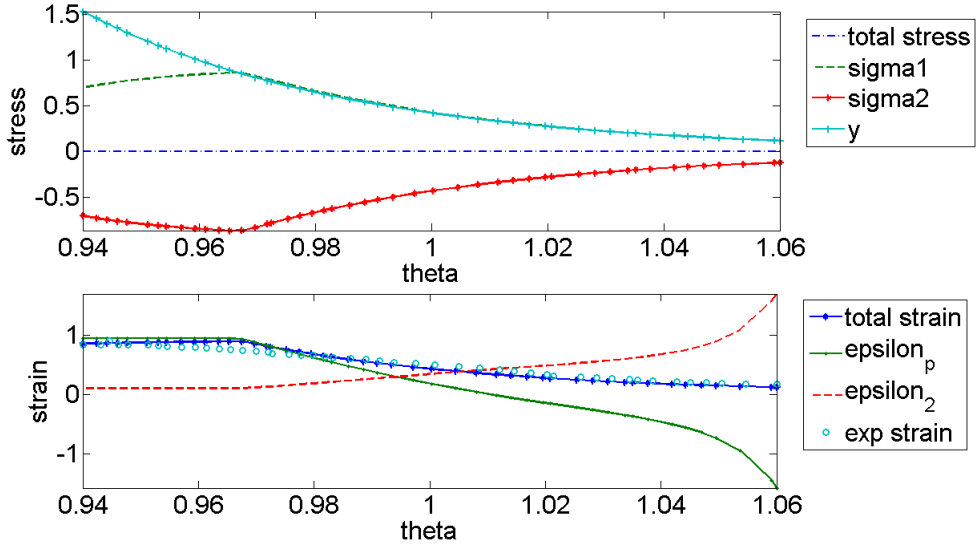

Fig. 33. Stress and strain in various elements of the model during Process D of heating at unstressed condition.

5. Process D:Heating the Material in Unstressed Condition

The material is now heated in unstressed condition and the resulting stress-strain response versus temperature is shown in Figure (33).

Thermal strain in the material is rising with increase in temperature. The yield-stress of the material is decreasing with increase in temperature. The plastic strain that was locked inside the material from previous region, gets unlocked as the the yield-stress of the material decreases to suitable value as can be seen in the figure at non-dimensional temperature value of around 0.97. The glassy spring modulus is reducing in this region and hence compressive stress in the temporary (glassy) network reduces in value, until it reaches that of the yield-stress of the friction damper. Once it does, the stress in the temporary network unlocks the dry friction damper, and the unlocked strain is now released. The locked-in strain in the friction damper is regained entirely. However, the stress in the temporary network continuously reduces

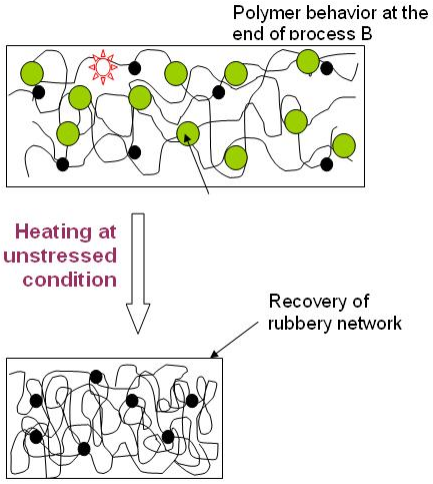

Fig. 34. Process D: Effect of heating in unstressed condition in polymer.

even after the strain in the network is zero, thus causing compression in the damper.

Physically, as shown in Figure (34), the heating causes the yield-stress of the material to fall, and hence reduces the stickiness of the material. The temporary nodes are not able to sustain as before, and start breaking at a fast rate again. Thus, their breakage sets the rubbery backbone of the material free, and it is able to coil back to almost its original configuration.

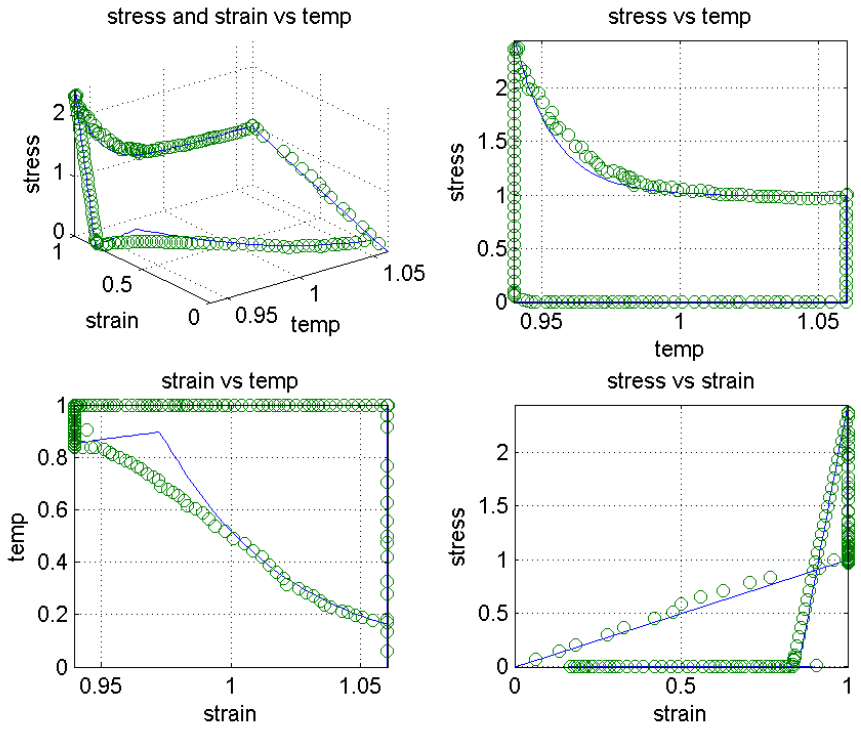

Fig. 35. Comparison of simulation results and experimental data.

C. Validation of Simulation

1. For $\epsilon_{max} = 2.4\%$

The results are compared with the experimental data obtained by Tobushi et al. [3] for $\epsilon_{max} = 2.4\%$ in Figure (35). Specifically, comparisons are made between figures 5,6, and 7 in Tobushi et al. In each case, there are variations in the quantitative shape of the curves but the non-dimensional values indicate quite good agreement.

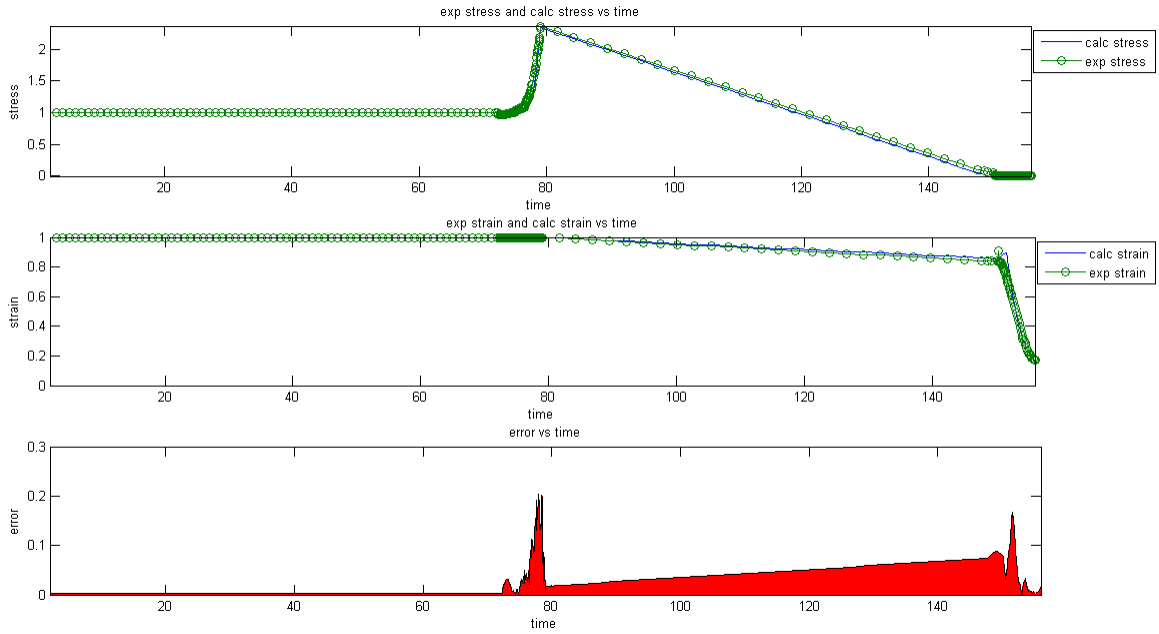

Fig. 36. Error between experimental and model.

Refer to figure (36). The results are compared with the experimental data obtained by Tobushi et. al. [3] in the figure and an absolute difference in the values is computed for error evaluation. The model gives significantly better results than those generated by the model proposed by Tobushi, because of the consideration of variation of mechanical properties with temperature change. The error is evident in the areas where temperature changes are occurring which highlight the fact that the form of dependence of the mechanical properties with temperature considered here, need to be specified more accurately.

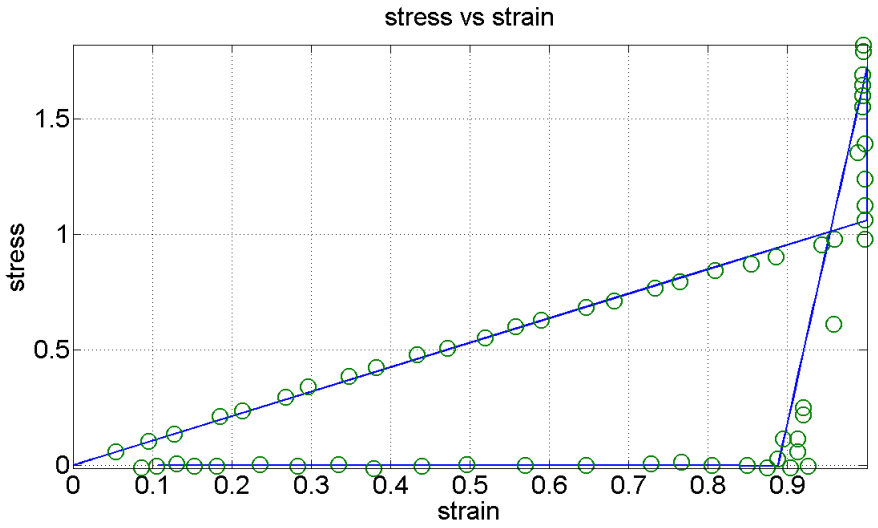

Fig. 37. Comparison of experimental and model results for $\epsilon_{max} = 4\%$.

2. For $\epsilon_{max} = 4\%$

The plot for $\epsilon_{max} = 4\%$ in Figure (37) shows qualitative matches in the trends of stress rise and strain recovery. End-of-zone values for each process are in quantitative agreement, which says for small maximum strains upto 4%, the model works well.

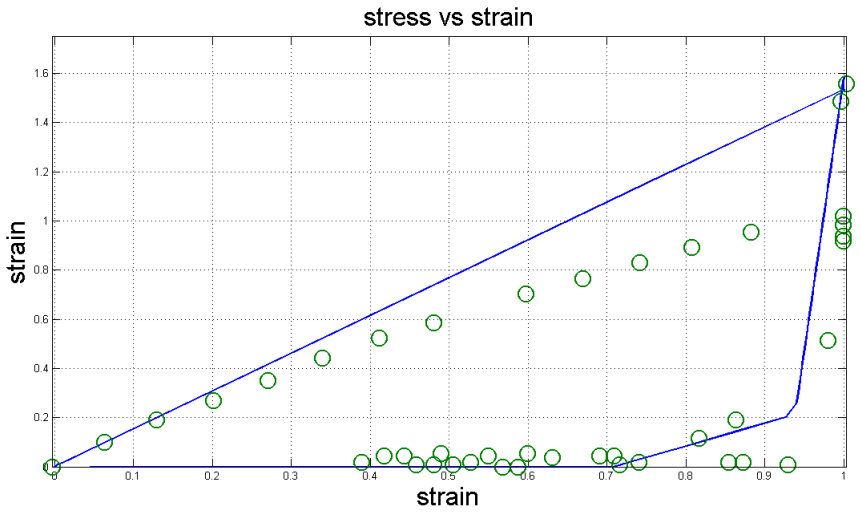

Fig. 38. Comparison of experimental and model results for $\epsilon_{max} = 10\%$.

3. For $\epsilon_{max} = 10\%$

The plot for $\epsilon_{max} = 10\%$ in Figure (38) shows that the model has non-linear response after a maximum strain of around 4%. Since we considered the stress to be a linear function of strain for this model, it does not work for large strains like 10% in above figure. The model fits for a linear response with the elastic modulus computed from strain of 2.4%. For non-linear responses, we shall have to consider higher-order response functions of the Helmholtz potential.

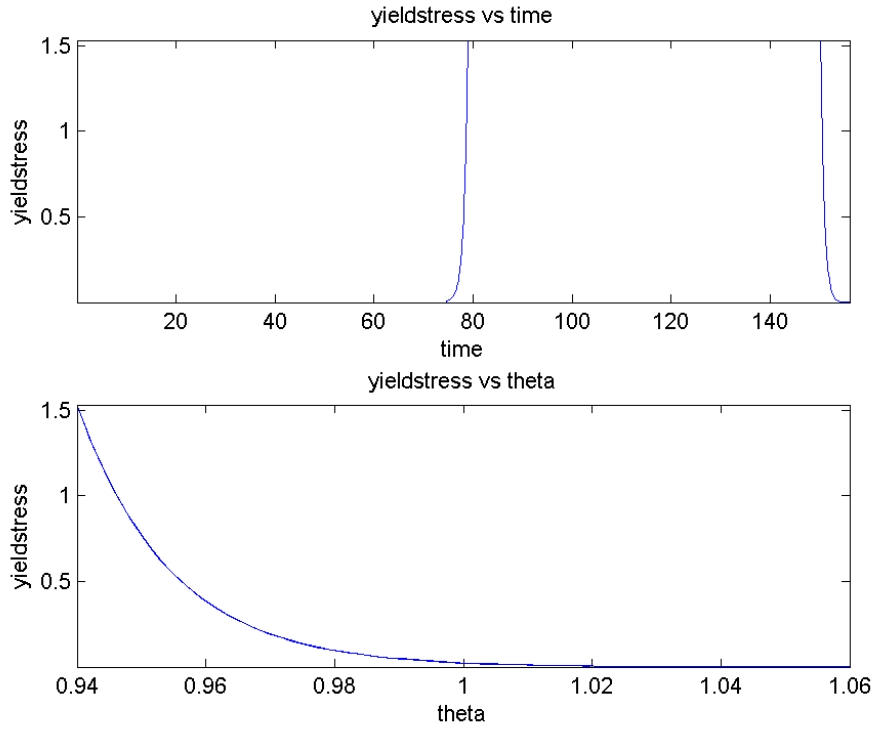

Fig. 39. Similar trend of yield-stress during heating and cooling.

D. Effect of the Yield-stress

1. Same Effect During Heating and Cooling

The key to the response of the material is the temperature dependence of the yield stress of the friction damper. Specifically, we suppose that $\hat{k}(\theta)$ is such that it is almost zero above the glass transition temperature θ_g and rises rapidly through the glass transition temperature to a much higher value when the temperature becomes below θ_g [30]. This gives results as shown in figure(40). As can be seen, the strain recovery process in Figure(40c) is drastically different from the material response observed in the experiment.

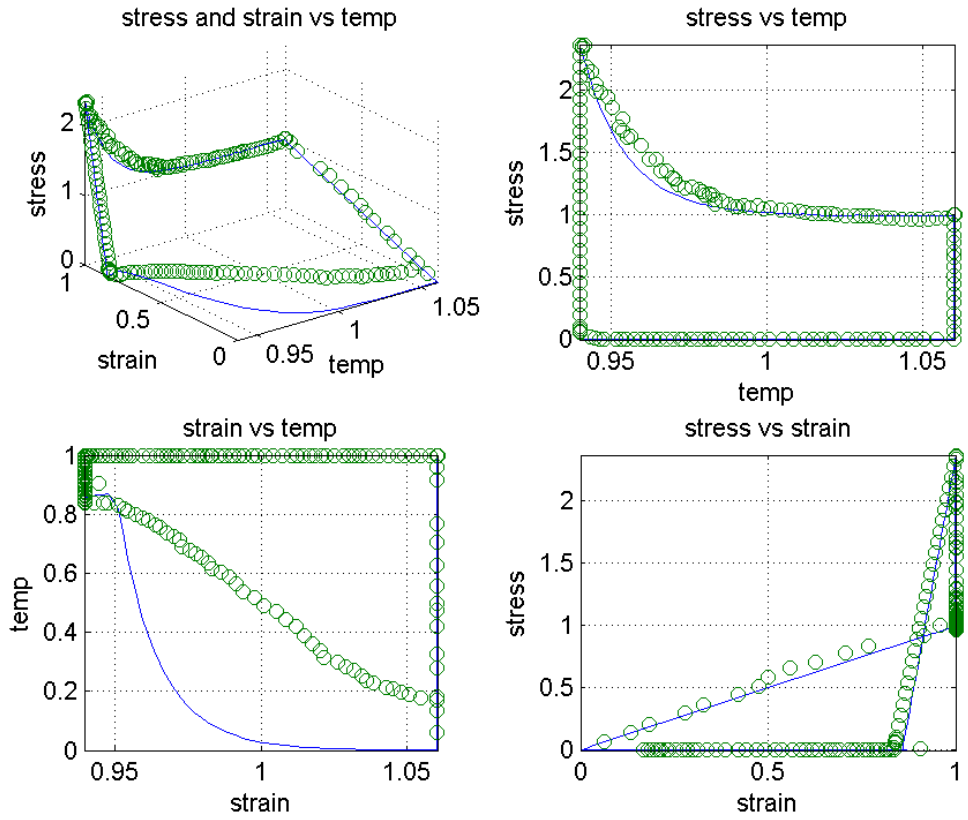

Fig. 40. Experimental results with similar yield-stress behavior for heating and cooling.

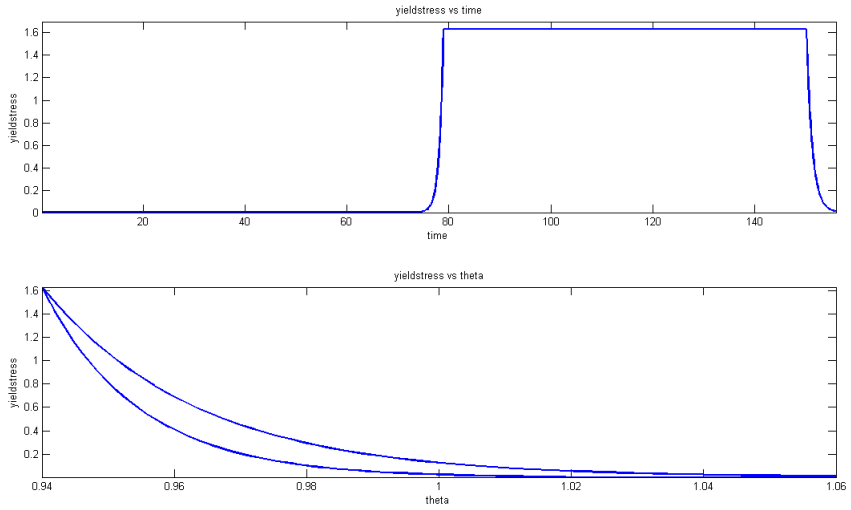

Fig. 41. Trend of yield-stress during heating and cooling.

2. Different Effects During Heating and Cooling

To overcome this deviation, the temperature dependence of the yield-stress is proposed to be different for heating and cooling processes as shown in the Figure (41). The rate of number of nodes that are broken and reformed is different in heating and cooling which affects the total recovery of the shape memory polymer. This rate is represented by the trend of yield-stress in the heating and cooling region. As opposed to the previous proposition of same behavior of yield-stress during heating and cooling in figure (39), if we consider a different behavior of the yield-stress during heating and cooling as shown in figure (41), we get results as shown in Figure (42). The yield-stress is thus proposed to have a functional form as

$$\dot{k} = \begin{cases} \frac{df_1(\theta)}{d\theta}\frac{d\theta}{dt}, & \frac{d\theta}{dt} > 0; \\ \frac{df_2(\theta)}{d\theta}\frac{d\theta}{dt}, & \frac{d\theta}{dt} < 0; \end{cases} \tag{5.1}$$

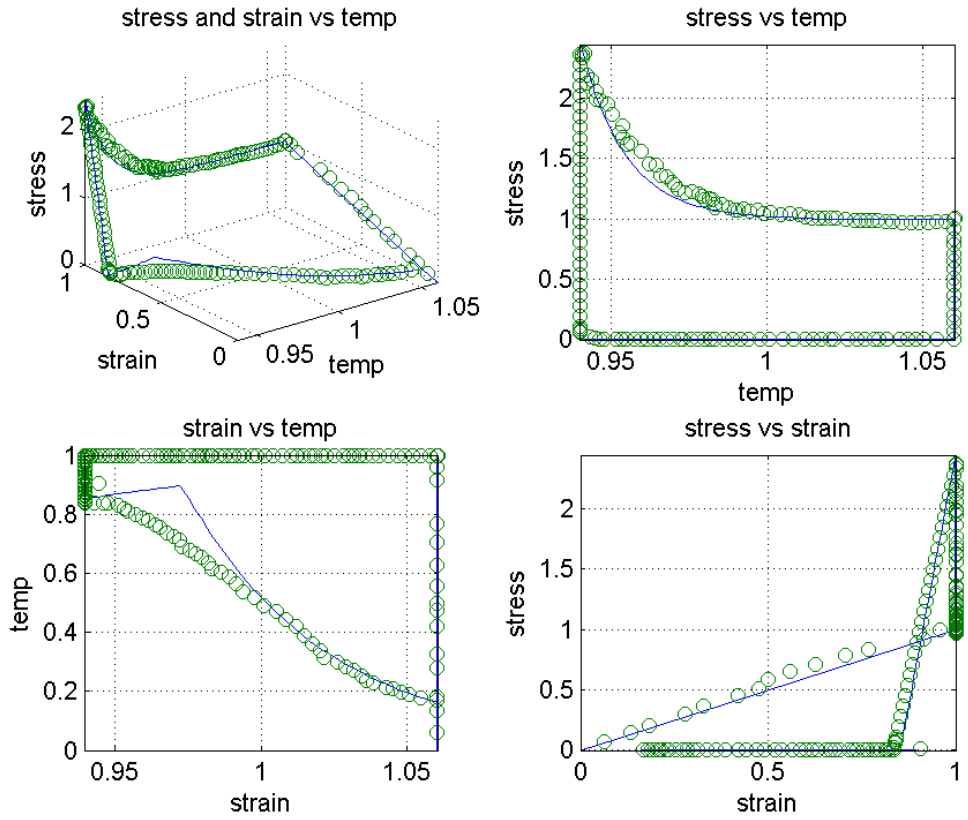

Fig. 42. Comparison of simulation results and experimental data.

The return of the strain during heating process significantly improves in this case, which leads us to believe that the hypothesis is correct.

CHAPTER VI

CONCLUSION

A. Further Work

The results of the error calculation as computed in the previous chapter, between the simulation results and the experimental data, shows clearly that the areas where temperature changes are occurring need to have a better response function. This highlights the fact that the form of dependence of the mechanical properties with temperature considered here, need to be specified more carefully.

In this work, the yield-stress of the material is varied for the heating and cooling processes, and it is suggested to affect the rate of temporary-junctions breaking and reforming in the cross-linked polymer matrix. This leads us to the next idea of whether the yield-stress at the end of the heating process will return to its initial value in the cooling process. Different return-values of the yield-stress shall be considered and its effect on the shape-recovery shall be monitored.

On a similar note, besides the rate of temporary-junctions breaking and reforming, it would be interesting to take into consideration the number of temporary-junctions created during heating and cooling process. This means the modulus of the material shall be different functions of temperature during heating and cooling which shall help in improving the simulated material response. This however, will have a bearing on the Helmholtz potential and hence will have to be studied carefully with thermodynamical consistency.

The present work was limited to keeping the Helmholtz potential as a quadratic function of the strain response of the material here, which led to unsatisfactory matches in the large-deformation experiments. A future model shall explore a cu-

bic or higher-order response function, and it is proposed that this shall meet the experimental data for $\epsilon_{max} = 10\%$ in a satisfactory manner.

The temperature of polymer is assumed to be the same as the ambient temperature in this experiment. Our next step shall be consideration of ambient temperatures through the heat equation.

Explicit history dependence of the material response, and moisture absorbtion capabilities of the material are also areas that remain to be explored. Appending the feature of moisture absorbtion in the material could make for a comprehensive model which is capable of shape changes, is thermally responsive and has moisture permeability as well.

B. Conclusion

The current work deals with the development of a thermodynamically consistent model for the response of a shape memory polyurethane-polypol sample undergoing a thermomechanical cycle. The system of model equations developed here was simulated in MATLAB and its results were shown to be in qualitative and quantitative agreement with experiments performed on polyurethane. We also showed here that most of the gross features of a SMP depend on the yield-stress of the material and we studied its dependence on temperature to be similar and different functions of heating or cooling processes.

REFERENCES

[1] S. Kelch and A. Lendlein, "Shape memory polymers," *Angew. Chem. Int. Edn Engl*, vol. 41, pp. 2034–2057, 2002.

[2] H. Tobushi, H. Hara, E. Yamada, and S. Hayashi, "Thermomechanical properties in a thin film of shape memory polymer of polyurethane series," *Smart Materials & Structures*, vol. 5, no. 4, pp. 483–491, 1996.

[3] H. Tobushi, T. Hashimoto, S. Hayashi, and E. Yamada, "Thermomechanical constitutive modeling in shape memory polymer of polyurethane series," *Journal of Intelligent Material Systems and Structures*, vol. 8, no. 8, pp. 711–718, 1997.

[4] H. Tobushi, T. Hashimoto, N. Ito, S. Hayashi, and E. Yamada, "Shape fixity and shape recovery in a film of shape memory polymer of polyurethane series," *Journal of Intelligent Material Systems and Structures*, vol. 9, no. 2, pp. 127–136, 1998.

[5] H. Tobushi, S. Hayashi, K. Hoshio, and Y. Ejiri, "Shape recovery and irrecoverable strain control in polyurethane shape-memory polymer," *Science and Technology of Advanced Materials*, vol. 9, no. 1, pp. 015009–015016, 2008.

[6] E.R. Abrahamson, M.S. Lake, N.A. Munshi, and K. Gall, "Shape memory mechanics of an elastic memory composite resin," *Journal of Intelligent Material Systems and Structures*, vol. 14, no. 10, pp. 623–632, 2003.

[7] T. Takahashi, N. Hayashi, and S. Hayashi, "Structure and properties of shape-memory polyurethane block copolymers," *Journal of Applied Polymer Science*, vol. 60, no. 7, pp. 1061–1069, 1996.

[8] S.H. Lee, J.W. Kim, and B.K. Kim, "Shape memory polyurethanes having crosslinks in soft and hard segments," *Smart Materials and Structures*, vol. 13, no. 6, pp. 1345–1350, 2004.

[9] J.R. Lin and L.W. Chen, "Shape-memorized crosslinked ester-type polyurethane and its mechanical viscoelastic model," *Journal of Applied Polymer Science*, vol. 73, no. 7, pp. 1305–1319, 1999.

[10] A. Bhattacharyya and H. Tobushi, "Analysis of the isothermal mechanical response of a shape memory polymer rheological model," *Polymer Engineering and Science*, vol. 40, no. 12, pp. 2498–2510, 2000.

[11] S.J. Hong, W.R. Yu, and J.H. Youk, "Thermomechanical deformation analysis of shape memory polymers using viscoelasticity," in *AIP Conference Proceedings*. AIP, 2007, vol. 907, pp. 853–858.

[12] Y. Liu, K. Gall, M.L. Dunn, A.R. Greenberg, and J. Diani, "Thermomechanics of shape memory polymers: Uniaxial experiments and constitutive modeling," *International Journal of Plasticity*, vol. 22, no. 2, pp. 279–313, 2006.

[13] J. Diani, Y. Liu, and K. Gall, "Finite strain 3D thermoviscoelastic constitutive model for shape memory polymers," *Polymer Engineering and Science*, vol. 46, no. 4, pp. 486, 2006.

[14] A. Lendlein and R. Langer, "Biodegradable, elastic shape-memory polymers for potential biomedical applications," *Science*, vol. 296, no. 5573, pp. 1673–1676, 2002.

[15] Q.Q. Ni, C. Zhang, Y. Fu, G. Dai, and T. Kimura, "Shape memory effect and

mechanical properties of carbon nanotube/shape memory polymer nanocomposites," *Composite Structures*, vol. 81, no. 2, pp. 176–184, 2007.

[16] J. Hu, "New Developments in elastic fibers," *Polymer Reviews*, vol. 48, no. 2, pp. 275–301, 2008.

[17] C. Liu, H. Qin, and P.T. Mather, "Review of progress in shape-memory polymers," *Journal of Materials Chemistry*, vol. 17, no. 16, pp. 1543–1558, 2007.

[18] J.L. Hu, *Shape Memory Polymers and Textiles*, Cambridge, Woodhead Publishing Ltd., 2007.

[19] K.P. Chong, S.C. Liu, and JC Li, *Intelligent Structures*, Oxford, Elsevier Applied Science, 1990.

[20] F. Li and R.C. Larock, "New soybean oil-styrene-divinylbenzene thermosetting copolymers. V. Shape memory effect," *Journal of Applied Polymer Science*, vol. 84, no. 8, pp. 1533–1543, 2002.

[21] V.A. Beloshenko, V.N. Varyukhin, and Y.V. Voznyak, "The shape memory effect in polymers," *Russian Chemical Reviews*, vol. 74, no. 3, pp. 265–283, 2005.

[22] A.S. Wineman and K.R. Rajagopal, *Mechanical Response of Polymers: An Introduction*, Cambridge, Cambridge University Press, 2000.

[23] D.R. Bland, *The Theory of Linear Viscoelasticity*, London, Pergamon, 1960.

[24] J. D. Ferry, *Viscoelastic Properties of Polymers (ed.)*, New York, Wiley, 1980.

[25] A.V. Tobolsky and R.D. Andrews, "Systems manifesting superposed elastic and viscous behavior," *The Journal of Chemical Physics*, vol. 13, pp. 3–27, 1945.

[26] A. R. Srinivasa and P. Ghosh, "A simple Gibb's Potential based multinetwork model for shape memory polymers," *Conference paper presented at IIT Madras, India*, 2008.

[27] A. R. Srinivasa, *Inelasticity of Materials: An Engineering Approach and Practical Guide*, Virgin Islands, World Scientific (To be published), 2009.

[28] Herbert. B Callen, *Thermodynamics and An Introduction to Thermostatistics*, New York, John Wiley & Sons, 1985.

[29] L.A. Segel and G.H. Handelman, *Mathematics Applied to Continuum Mechanics*, New York, Dover Publications, 1987.

[30] J. Richeton, S. Ahzi, L. Daridon, and Y. Rémond, "A formulation of the cooperative model for the yield stress of amorphous polymers for a wide range of strain rates and temperatures," *Polymer*, vol. 46, no. 16, pp. 6035–6043, 2005.

VITA

Pritha Ghosh

Department of Mechanical Engineering, Texas A&M University, D-08

College Station, TX 77843-3123.

Education

Dec '08: *M.S Mechanical Engineering*, Texas A&M University, College Station, TX.

Aug '05: *B.E Mechanical Engineering*, Govt. College of Engineering Pune, India.

Experience

June '05 to July '06 : *Design Engineer*, Tata Technologies Ltd, Hinjewadi-Pune, India

Fall '06 : *Student Worker*, MSC Dining Services, Texas A&M University, College Station, TX.

Spring '07 : *Student Worker*, Mechanical Engg Dept., Texas A&M University, College Station, TX.

Summer '07 - Fall '08: *Graduate Assistant Non-Teaching*, Texas A&M University, College Station, TX.